Allyl Carborane Complexes of Molybdenum and Tungsten: Cage–Hydride Abstraction Reactions in the Presence of Donor Molecules

Donald F. Mullica, Eric L. Sappenfield, F. Gordon A. Stone,[*] and Stephen F. Woollam

Department of Chemistry, Baylor University, Waco, Texas 76798-7348

Received September 27, 1993[•]

Treatment of the salts $[NEt_4][Mo(CO)_2(\eta^3\text{-}C_3H_5)(\eta^5\text{-}7,8,\text{-}R'_2\text{-}7,8\text{-}C_2B_9H_9)]$[†] (R′ = H (**1a**) or Me (**1b**)) in CH_2Cl_2 with $[CPh_3][BF_4]$ in the presence of donor molecules L affords the complexes $[Mo(CO)_2(\eta^3\text{-}C_3H_5)(\eta^5\text{-}7,8\text{-}R'_2\text{-}7,8\text{-}C_2B_9H_8\text{-}10\text{-}L)]$ (R′ = H, L = OEt_2 (**2a**); R′ = Me, L = OEt_2 (**2b**), thf (tetrahydrofuran) (**2d**), SMe_2 (**2e**), PPh_3 (**2f**), NC_5H_5 (**2g**), or 4,4′-$NC_5H_4C_5H_4N$ (**2h**)). The tungsten compound $[W(CO)_2(\eta^3\text{-}C_3H_5)(\eta^5\text{-}7,8\text{-}Me_2\text{-}7,8\text{-}C_2B_9H_8\text{-}10\text{-}OEt_2)]$ (**2c**) has been similarly prepared from $[NEt_4][W(CO)_2(\eta^3\text{-}C_3H_5)(\eta^5\text{-}7,8\text{-}Me_2\text{-}7,8\text{-}C_2B_9H_9)]$ (**1c**). The structure of **2b** has been established by X-ray crystallography. Crystals are triclinic, space group $P\bar{1}$ (No. 2) with a = 7.106(1) Å, b = 9.088(2) Å, c = 16.271(2) Å, α = 75.08(1)°, β = 92.77(1)°, γ = 102.19(1)°, and Z = 2. The molybdenum atom is ligated on one side by two essentially linearly bound CO molecules and the allyl group, the latter adopting an η^3-bonding mode (Mo–C = 2.342(4), 2.234(4), and 2.365(4) Å). On the other side, the molybdenum atom is coordinated by the open pentagonal face of the *nido*-7,8-C_2B_9 fragment. The boron atom in this face which is in the β-site with respect to the two carbons carries an OEt_2 molecule as an exopolyhedral substituent (B–O = 1.544(3) Å). Thus, **2b** is a zwitterionic complex with formally a plus charge on the oxygen atom and a negative charge on the molybdenum atom. Treatment of CH_2Cl_2 solutions of **2b** and **2c**, respectively, with $K[BH\{CH(Me)(Et)\}_3]$, followed by addition of $[NEt_4]Cl$, affords the species $[NEt_4][M(CO)_2(\eta^3\text{-}C_3H_5)(\eta^5\text{-}7,8\text{-}Me_2\text{-}7,8\text{-}C_2B_9H_8\text{-}10\text{-}OEt)]$ (M = Mo (**3a**) and W (**3b**)). Similarly, treatment of tetrahydrofuran solutions of **2b**–**2d** with $[NEt_4]F$ gives the salts **3a**, **3b**, and $[NEt_4][Mo(CO)_2(\eta^3\text{-}C_3H_5)\{\eta^5\text{-}7,8\text{-}Me_2\text{-}7,8\text{-}C_2B_9H_8\text{-}10\text{-}O(CH_2)_3CH_2F\}]$ (**3c**), respectively. Protonation ($HBF_4{\cdot}Et_2O$) of the species **3**, in CO-saturated CH_2Cl_2 solutions, yields the complexes $[M(CO)_4(\eta^5\text{-}7,8\text{-}Me_2\text{-}7,8\text{-}C_2B_9H_8\text{-}10\text{-}OEt)]$ (M = Mo (**4a**), W (**4c**)) and $[Mo(CO)_4\{\eta^5\text{-}7,8\text{-}Me_2\text{-}7,8\text{-}C_2B_9H_8\text{-}10\text{-}O(CH_2)_3CH_2F\}]$ (**4d**), respectively. In CH_2Cl_2 solutions at room temperature, compound **4a** slowly converts to its polytopal isomer $[Mo(CO)_4(\eta^5\text{-}2,8\text{-}Me_2\text{-}2,8\text{-}C_2B_9H_8\text{-}10\text{-}OEt)]$ (**4b**). Complexes **4a** and **4b** react with $[W(\equiv CC_6H_4Me\text{-}4)(CO)_2(\eta^5\text{-}C_5H_5)]$ in CH_2Cl_2 to give, respectively, the isomeric dimetal compounds $[MoW(\mu\text{-}CC_6H_4Me\text{-}4)(CO)_3(\eta^5\text{-}C_5H_5)(\eta^5\text{-}n,8\text{-}Me_2\text{-}n,8\text{-}C_2B_9H_8\text{-}10\text{-}OEt)]$ (n = 7, **6a**; n = 2, **6b**). The structure of **6b** has been established by X-ray crystallography. Crystals are monoclinic, space group $C2/c$ (No. 15) with a = 28.763(3) Å, b = 10.950(3) Å, c = 18.030(1) Å, β = 94.785(7)°, and Z = 8. The Mo–W bond (2.645(1) Å) is spanned by the *p*-tolylmethylidyne group (μ-C–Mo = 2.088(7) Å, μ-C–W = 1.961(7) Å). The tungsten atom as expected carries the C_5H_5 ring and a CO molecule, while the molybdenum atom is coordinated by two CO groups and is also bonded to the five atoms in the open CBBBB face of the carborane cage, forming with the latter an icosahedral 2,1,8-MoC_2B_9 framework. A boron atom β to the carbon in the CBBBB ring ligating the molybdenum carries the OEt substituent (B–O = 1.41(1) Å), and the BH vertex between the BOEt and CMe vertices forms an exopolyhedral B–H ⇀ W linkage (B–W = 2.415(9) Å, μ-H–B = 1.11 Å, μ-H–W = 1.87 Å). The new complexes have been characterized by IR and NMR spectroscopy, in addition to the X-ray diffraction studies.

Introduction

We have recently reported the synthesis of the complexes $[Y][M(CO)_2(\eta^3\text{-}C_3H_5)(\eta^5\text{-}7,8\text{-}R'_2\text{-}7,8\text{-}C_2B_9H_9)]$ (Y = $[N(PPh_3)_2]^+$ or $[NEt_4]^+$, M = Mo or W, R′ = H or Me) and have begun to explore their chemistry.[1] The anions of these salts are isolobal with the neutral complexes $[M(CO)_2(\eta^3\text{-}C_3H_5)(\eta^5\text{-}C_5H_5)]$. Because the latter have long been useful synthons in organomolybdenum and -tungsten chemistry,[2] it is to be anticipated that the carborane species will also function as sources of new complexes of these metals, with the probability that in some reactions the carborane cage will adopt a nonspectator role, thereby affording products with unusual molecular structures.[3]

---

[*] To whom correspondence should be addressed.

[†] In the compounds described in this paper, molybdenum or tungsten atoms and *nido*-C_2B_9 cages form *closo*-1,2-dicarba-3-metalladodecaborane structures. However, use of this numbering scheme leads to an impossibly complex nomenclature for the metal complexes reported. Following precedent (Carr, N.; Mullica, D. F.; Sappenfield, E. L.; Stone, F. G. A. *Organometallics* **1992**, *11*, 3697), we therefore treat the cages as *nido* 11-vertex ligands with numbering as for an icosahedron from which the twelfth vertex has been removed.

[•] Abstract published in *Advance ACS Abstracts*, December 1, 1993.

(1) (a) Dossett, S. J.; Li, S.; Stone, F. G. A. *J. Chem. Soc., Dalton Trans.* **1993**, 1585. (b) Li, S.; Stone, F. G. A. *Polyhedron* **1993**, *12*, 1689. (c) Dossett, S. J.; Li, S.; Mullica, D. F.; Sappenfield, E. L.; Stone, F. G. A. *J. Chem. Soc., Dalton Trans.* **1993**, 3551.

(2) Davis, R.; Kane-Maguire, L. A. P. In *Comprehensive Organometallic Chemistry*; Wilkinson, G., Stone, F. G. A., Abel, E. W., Eds.; Pergamon: Oxford, 1982; Vol. 3, pp 1159–1163, 1327–1328.

0276-7333/94/2313-0157$04.50/0

Table 1. Physical and Infrared Absorption Data

compd		color	yield/%	$\nu_{max}(CO)^a/cm^{-1}$	anal.[b]/% C	anal.[b]/% H
2a	$[Mo(CO)_2(\eta^3\text{-}C_3H_5)(\eta^5\text{-}7,8\text{-}C_2B_9H_{10}\text{-}10\text{-}OEt_2)]$	yellow	72	1940vs, 1854s	33.1 (33.2)	6.6 (6.3)
2b	$[Mo(CO)_2(\eta^3\text{-}C_3H_5)(\eta^5\text{-}7,8\text{-}Me_2\text{-}7,8\text{-}C_2B_9H_8\text{-}10\text{-}OEt_2)]$	yellow	68	1938vs, 1851s	36.6 (36.5)	7.3 (7.1)
2c	$[W(CO)_2(\eta^3\text{-}C_3H_5)(\eta^5\text{-}7,8\text{-}Me_2\text{-}7,8\text{-}C_2B_9H_8\text{-}10\text{-}OEt_2)]$	yellow	75	1931vs, 1843s	30.9 (30.3)	5.8 (5.7)
2d	$[Mo(CO)_2(\eta^3\text{-}C_3H_5)(\eta^5\text{-}7,8\text{-}Me_2\text{-}7,8\text{-}C_2B_9H_8\text{-}10\text{-}OC_4H_8)]$	yellow	68	1936vs, 1848s	36.9 (36.8)	7.0 (6.4)
2e	$[Mo(CO)_2(\eta^3\text{-}C_3H_5)(\eta^5\text{-}7,8\text{-}Me_2\text{-}7,8\text{-}C_2B_9H_8\text{-}10\text{-}SMe_2)]$	yellow	37	1940vs, 1852s	33.3 (31.9)	6.1 (6.1)
2f	$[Mo(CO)_2(\eta^3\text{-}C_3H_5)(\eta^5\text{-}7,8\text{-}Me_2\text{-}7,8\text{-}C_2B_9H_8\text{-}10\text{-}PPh_3)]$	orange	44	1938vs, 1853s	52.8 (52.8)	6.0 (5.6)
2g	$[Mo(CO)_2(\eta^3\text{-}C_3H_5)(\eta^5\text{-}7,8\text{-}Me_2\text{-}7,8\text{-}C_2B_9H_8\text{-}10\text{-}NC_5H_5)]$	yellow	45	1937vs, 1851s	39.6 (39.0)[c]	6.3 (5.6)
2h	$[Mo(CO)_2(\eta^3\text{-}C_3H_5)(\eta^5\text{-}7,8\text{-}Me_2\text{-}7,8\text{-}C_2B_9H_8\text{-}10\text{-}NC_5H_4C_5H_4N)]$	orange	34	1937vs, 1852s	45.0 (44.9)[d]	5.1 (5.4)
3a	$[NEt_4][Mo(CO)_2(\eta^3\text{-}C_3H_5)(\eta^5\text{-}7,8\text{-}Me_2\text{-}7,8\text{-}C_2B_9H_8\text{-}10\text{-}OEt)]$	yellow	73	1916vs, 1824s	43.5 (43.2)[e]	8.5 (8.4)
3b	$[NEt_4][W(CO)_2(\eta^3\text{-}C_3H_5)(\eta^5\text{-}7,8\text{-}Me_2\text{-}7,8\text{-}C_2B_9H_8\text{-}10\text{-}OEt)]$	yellow	66	1906vs, 1813s	37.1 (37.1)[f]	6.9 (7.2)
3d	$[NBu^n{}_4][Mo(CO)_2(\eta^3\text{-}C_3H_5)\{\eta^5\text{-}7,8\text{-}Me_2\text{-}7,8\text{-}C_2B_9H_8\text{-}10\text{-}O(CH_2)_3CH_2F\}]$	yellow	60	1916vs, 1826s	51.2 (50.8)[g]	9.9 (9.3)
4a	$[Mo(CO)_4(\eta^5\text{-}7,8\text{-}Me_2\text{-}7,8\text{-}C_2B_9H_8\text{-}10\text{-}OEt)]$[h]	yellow	43	2096vs, 2037sh 2012vs		
4b	$[Mo(CO)_4(\eta^5\text{-}2,8\text{-}Me_2\text{-}2,8\text{-}C_2B_9H_8\text{-}10\text{-}OEt)]$[h]	yellow	20	2096s, 2035sh 2010vs		
4c	$[W(CO)_4(\eta^5\text{-}7,8\text{-}Me_2\text{-}7,8\text{-}C_2B_9H_8\text{-}10\text{-}OEt)]$	yellow	55	2096vs, 2029sh 2002vs	23.9 (24.0)	3.8 (3.8)
4d	$[Mo(CO)_4\{\eta^5\text{-}7,8\text{-}Me_2\text{-}7,8\text{-}C_2B_9H_8\text{-}10\text{-}O(CH_2)_3CH_2F\}]$[h]	yellow	44	2097s, 2037sh 2012vs		
6a	$[MoW(\mu\text{-}CC_6H_4Me\text{-}4)(CO)_3(\eta^5\text{-}C_5H_5)(\eta^5\text{-}7,8\text{-}Me_2\text{-}7,8\text{-}C_2B_9H_8\text{-}10\text{-}OEt)]$	green	45	2005vs, 1955vs 1933sh	36.4 (35.9)	4.4 (4.2)
6b	$[MoW(\mu\text{-}CC_6H_4Me\text{-}4)(CO)_3(\eta^5\text{-}C_5H_5)(\eta^5\text{-}2,8\text{-}Me_2\text{-}2,8\text{-}C_2B_9H_8\text{-}10\text{-}OEt)]$	green	35	2002vs, 1948vs 1936sh	36.5 (35.9)	4.2 (4.2)

[a] Measured in CH_2Cl_2. All complexes show a weak, very broad absorption at ca. 2550 cm^{-1} due to cage B–H stretches. [b] Calculated values are given in parentheses. [c] N, 3.0 (3.2). [d] N, 5.3 (5.5). [e] N, 2.7 (2.7). [f] N, 2.3 (2.3). [g] N, 2.3 (2.0). [h] Product insufficiently stable to obtain suitable microanalyses, see text.

Thus, protonation ($HBF_4{\cdot}Et_2O$) of CO-saturated CH_2Cl_2 solutions of $[N(PPh_3)_2][Mo(CO)_2(\eta^3\text{-}C_3H_5)(\eta^5\text{-}7,8\text{-}Me_2\text{-}7,8\text{-}C_2B_9H_9)]$ results in elimination of the allyl group as $MeCH{=}CH_2$ and formation of $[Mo(CO)_4(\eta^5\text{-}7,8\text{-}Me_2\text{-}7,8\text{-}C_2B_9H_9)]$, a complex in which the cage adopts a spectator role.[1a] In contrast, a similar protonation reaction of this salt in the presence of $Me_3SiC{\equiv}CH$, although yielding initially $[Mo(CO)(\eta^2\text{-}Me_3SiC_2H)_2(\eta^5\text{-}7,8\text{-}Me_2\text{-}7,8\text{-}C_2B_9H_9)]$, gives as the end product $[Mo(CO)(\eta^2\text{-}Me_3SiC_2H)\{\eta^2,\eta^5\text{-}7,8\text{-}Me_2\text{-}7,8\text{-}C_2B_9H_8\text{-}10\text{-}[CH{=}C(H)SiMe_3]\}]$ in which the cage carries a vinyl substituent.[1c]

In contrast with the protonation studies, we have now found that salts of the type $[Y][M(CO)_2(\eta^3\text{-}C_3H_5)(\eta^5\text{-}7,8\text{-}R'_2\text{-}7,8\text{-}C_2B_9H_9)]$ undergo facile hydride abstraction reactions upon treatment with the reagent $[CPh_3][BF_4]$,[4] and the results are described in this paper.

Results and Discussion

Addition of $[CPh_3][BF_4]$ to a CH_2Cl_2 solution of **1a** at −78 °C, in the presence of OEt_2, gives the complex $[Mo(CO)_2(\eta^3\text{-}C_3H_5)(\eta^5\text{-}7,8\text{-}C_2B_9H_{10}\text{-}10\text{-}OEt_2)]$ (**2a**). The related compounds **2b** and **2c** were similarly prepared from **1b** and **1c**, respectively. If the hydride abstraction reaction of **1b** is carried out in the presence of thf (tetrahydrofuran), SMe_2, PPh_3, NC_5H_5, or 4,4′-$NC_5H_4C_5H_4N$, the complexes $[Mo(CO)_2(\eta^3\text{-}C_3H_5)(\eta^5\text{-}7,8\text{-}Me_2\text{-}7,8\text{-}C_2B_9H_8\text{-}10\text{-}L)]$ (L = thf (**2d**), SMe_2 (**2e**), PPh_3 (**2f**), NC_5H_5 (**2g**), and 4,4′-$NC_5H_4C_5H_4N$ (**2h**)) are obtained. Data characterizing these compounds are given in Tables 1–3. However, the molecular structure of this class of complex was unequivocally established by a single-crystal X-ray analysis of **2b**.

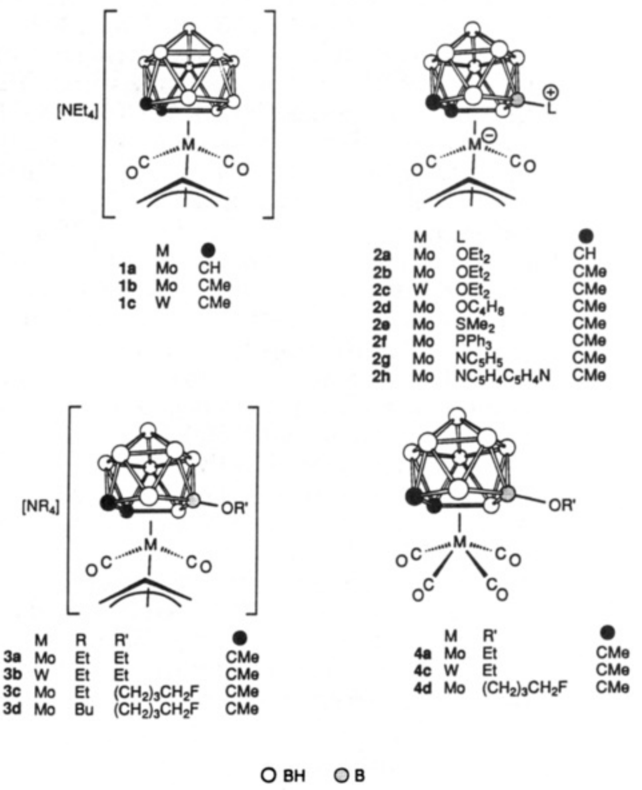

Selected structural parameters for **2b** are listed in Table 4, and the molecule is shown in Figure 1. The *nido*-C_2B_9 cage is coordinated to the molybdenum atom by the open CCBBB face in the usual pentahapto manner, but interest focuses on B(4), lying in the β-site with respect to the two carbon atoms. This boron atom is bonded to a diethyl ether molecule through the oxygen atom (B(4)–O(1) 1.544(3) Å), so the hydride abstraction process clearly involves the unique BH vertex in the η^5-C_2B_3 ring. Activation of this β-BH vertex of a *nido*-C_2B_9 cage, with replacement of the hydrogen substituent, has been previously observed in metallacarborane chemistry. Thus

---

(3) (a) Brew, S. A.; Stone, F. G. A. *Adv. Organomet. Chem.* **1993**, *35*, 135. (b) Stone, F. G. A. *Adv. Organomet. Chem.* **1990**, *31*, 53.

(4) Use of this reagent for removal of H^- is well documented. See, for example: Dauben, H. J.; Honnen, L. P. *J. Am. Chem. Soc.* **1958**, *80*, 5570. Hannon, S. J.; Traylor, T. G. *J. Org. Chem.* **1981**, *46*, 3645. Lambert, J. B.; Schulz, W. J. *J. Am. Chem. Soc.* **1983**, *105*, 1671. Markham, J.; Menard, K.; Cutler, A. *Inorg. Chem.* **1985**, *24*, 1581. Kegley, M.; Brookhart, M.; Husk, G. R. *Organometallics* **1982**, *1*, 760. Bodner, G. S.; Gladysz, J. A.; Nielsen, M. F.; Parker, V. D. *J. Am. Chem. Soc.* **1987**, *109*, 1757.

Table 2. Hydrogen-1 NMR Data[a]

compd[b]	^{1}H/δ
2a	1.40 (d, 2 H, H_a, $J(H_aH_c)$ = 9), 1.52 (t, 6 H, OCH$_2$*Me*, J(HH) = 7), 1.65 (s br, 2 H, cage CH), 3.27 to 3.33 (m, 3 H, H_c and H_s), 4.55 (q, 4 H, OC*H*$_2$Me, J(HH) = 7)
2b	1.22 (d of t, 2 H, H_a, $J(H_aH_c)$ = 11, $J(H_aH_s)$ = 1), 1.43 (t, 6 H, OCH$_2$*Me*, J(HH) = 7), 1.61 (s, 6 H, CMe), 3.07 (d of t, 2 H, H_s, $J(H_sH_c)$ = 7, $J(H_sH_a)$ = 1), 3.85 (t of t, 1 H, H_c, J(HH) = 11 and 7), 4.38 (q, 4 H, OC*H*$_2$Me, J(HH) = 7)
2c	1.40 (d of t, 2 H, H_a, $J(H_aH_c)$ = 10, $J(H_aH_s)$ = 1), 1.44 (t, 6 H, OCH$_2$*Me*, J(HH) = 7), 1.80 (s, 6 H, CMe), 3.02 (d of t, 2 H, H_s, $J(H_sH_c)$ = 7, $J(H_sH_a)$ = 1), 3.44 (t of t, 1 H, H_c, J(HH) = 10 and 7), 4.37 (q, 4 H, OC*H*$_2$Me, J(HH) = 7)
2d[c]	1.18 (d of t, 2 H, H_a, $J(H_aH_c)$ = 11, $J(H_aH_s)$ = 1), 1.72 (s, 6 H, CMe), 2.25 to 2.29 (m, 4 H, OCH$_2$C*H*$_2$), 3.21 (d of t, 2 H, H_s, $J(H_sH_c)$ = 7, $J(H_sH_a)$ = 1), 4.08 (t of t, 1 H, H_c, J(HH) = 11 and 7), 4.39 to 4.43 (m, 4 H, OCH$_2$)
2e	1.34 (d of t, 2 H, H_a, $J(H_aH_c)$ = 11, $J(H_aH_s)$ = 1), 1.75 (s, 6 H, CMe), 2.44 (s, 6 H, SMe), 3.18 (d of t, 2 H, H_s, $J(H_sH_c)$ = 7, $J(H_sH_a)$ = 1), 4.03 (t of t, 1 H, H_c, J(HH) = 11 and 7)
2f	0.69 (d, 2 H, H_a, $J(H_aH_c)$ = 10), 1.89 (s, 6 H, CMe), 2.27 (d, 2 H, H_s, $J(H_sH_c)$ = 7), 3.80 (t of t, 1 H, H_c, J(HH) = 10 and 7), 7.49 to 7.76 (m, 15 H, C_6H_5)
2g	1.13 (d of t, 2 H, H_a, $J(H_aH_c)$ = 10, $J(H_aH_s)$ = 1), 1.73 (s, 6 H, CMe), 2.92 (d of t, 2 H, H_s, $J(H_sH_c)$ = 7, $J(H_sH_a)$ = 1), 3.91 (t of t, 1 H, H_c, J(HH) = 10 and 7), 7.66 (t, 2 H, NCH, J(HH) = 7), 8.05 (t of t, 1 H, NCHCHC*H*, J(HH) = 7 and 1), 8.47 (d, 2 H, NCHC*H*, J(HH) = 7)
2h	1.17 (d of t, 2 H, H_a, $J(H_aH_c)$ = 11, $J(H_aH_s)$ = 1), 1.74 (s, 6 H, CMe), 2.95 (d of t, 2 H, H_s, $J(H_sH_c)$ = 7, $J(H_sH_a)$ = 1), 3.93 (t of t, 1 H, H_c, J(HH) = 11 and 7), 7.60 to 8.82 (m, 8 H, $NC_5H_4C_5H_4N$)
3a	1.00 (d, 2 H, H_a, $J(H_aH_c)$ = 11), 1.01 (t, 3 H, OCH$_2$*Me*, J(HH) = 7), 1.32 (t of t, 12 H, NCH$_2$*Me*, J(HH) = 7, J(NH) = 2), 2.05 (s, 6 H, CMe), 2.89 (d, 2 H, H_s, $J(H_sH_c)$ = 7), 3.14 (q, 2 H, OCH$_2$, J(HH) = 7), 3.21 (q, 8 H, NCH$_2$, J(HH) = 7), 4.21 (t of t, 1 H, H_c, J(HH) = 11 and 7)
3b	1.00 (t, 3 H, OCH$_2$*Me*, J(HH) = 7), 1.15 (d, 2 H, H_a, $J(H_aH_c)$ = 10), 1.28 (t of t, 12 H, NCH$_2$*Me*, J(HH) = 7, J(NH) = 2), 2.34 (s, 6 H, CMe), 2.81 (d, 2 H, H_s, $J(H_sH_c)$ = 7), 3.09 (q, 2 H, OCH$_2$, J(HH) = 7), 3.17 (q, 8 H, NCH$_2$, J(HH) = 7), 3.77 (t of t, 1 H, H_c, J(HH) = 10 and 7)
3d	1.00 (d, 2 H, H_a, $J(H_aH_c)$ = 11), 1.02 (t, 12 H, N(CH$_2$)$_3$*Me*, J(HH) = 7), 1.38 to 1.51 (m, 10 H, NCH$_2$CH$_2$C*H*$_2$ and OCH$_2$CH$_2$C*H*$_2$), 1.56 to 1.82 (m, 10 H, NCH$_2$C*H*$_2$ and OCH$_2$C*H*$_2$), 2.08 (s, 6 H, CMe), 2.92 (d, 2 H, H_s, $J(H_sH_c)$ = 7), 3.07–3.12 (m, 8 H, NCH$_2$), 3.14 (t, 2 H, OCH$_2$, J(HH) = 7), 4.21 (t of t, 1 H, H_c, J(HH) = 11 and 7), 4.43 (d of t, 2 H, CH$_2$F, J(FH) = 48, J(HH) = 6)
4a	1.01 (t, 3 H, OCH$_2$*Me*, J(HH) = 7), 2.22 (s, 6 H, CMe), 3.22 (q, 2 H, OCH$_2$, J(HH) = 7)
4b	1.04 (t, 3 H, OCH$_2$*Me*, J(HH) = 7), 1.51 (s, 3 H, CMe), 1.76 (s, 3 H, CMe), 3.30 (q, 2 H, OCH$_2$, J(HH) = 7)
4c	1.02 (t, 3 H, OCH$_2$*Me*, J(HH) = 7), 2.42 (s, 6 H, CMe), 3.23 (q, 2 H, OCH$_2$, J(HH) = 7)
4d	1.42 to 1.54 (m, 2 H, OCH$_2$CH$_2$C*H*$_2$), 1.58 to 1.73 (m, 2 H, OCH$_2$C*H*$_2$), 2.22 (s, 6 H, CMe), 3.19 (t, 2 H, OCH$_2$, J(HH) = 6), 4.39 (d of t, 2 H, CH$_2$F, J(FH) = 47, J(HH) = 6)
6a	−7.52 (q, br, 1 H, BHW, J(BH) = 60), 0.61 (t, 3 H, OCH$_2$*Me*, J(HH) = 7), 1.97 (s, 3 H, CMe), 2.19 (s, 3 H, CMe), 2.54 (s, 3 H, C$_6$H$_4$*Me*), 2.55 (q, 2 H, OCH$_2$, J(HH) = 7), 5.60 (s, 5 H, C_5H_5), 6.80, 7.38 {(AB)$_2$, 4 H, C_6H_4, J(AB) = 8}
6b	−8.27 (q, br, 1 H, BHW, J(BH) = 61), 0.60 (t, 3 H, OCH$_2$*Me*, J(HH) = 7), 1.57 (s, 6 H, CMe), 1.91 (s, 6 H, CMe), 2.47 {(ABC$_3$), 2 H, OCH$_2$, J(AB) = 10, J(AC) = J(BC) = 7}, 2.54 (s, 3 H, C$_6$H$_4$*Me*), 5.59 (s, 5 H, C_5H_5), 6.82, 7.36 {(AB)$_2$, 4 H, C_6H_4, J(AB) = 8}

[a] Measured in CD_2Cl_2 at ambient temperatures, unless otherwise stated. *J* values given in Hz. Proton resonances for terminal B–H groups occur as broad unresolved peaks in the range δ *ca.* −2 to +3 ppm. [b] In the complexes with an allyl ligand, H_a, H_c, and H_s refer to the protons:

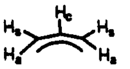

[c] Measured in acetone-d_6.

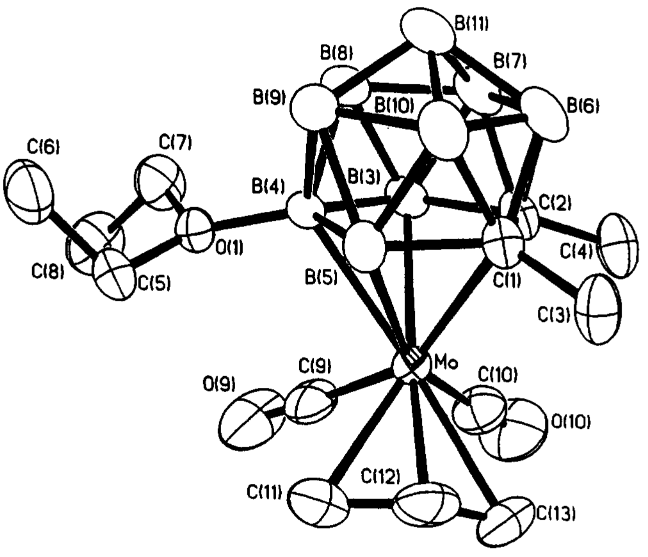

Figure 1. Structure of [Mo(CO)$_2$(η^3-C$_3$H$_5$)(η^5-7,8-Me$_2$-7,8-C$_2$B$_9$H$_8$-10-OEt$_2$)] (**2b**), showing the crystallographic labeling scheme.

the anionic species [FeH(η^5-7,8-C$_2$B$_9$H$_{11}$)$_2$]$^-$ undergoes electrophilic substitution on reaction with SEt$_2$, with release of hydrogen, to give [Fe(η^5-7,8-C$_2$B$_9$H$_{11}$)(η^5-7,8-C$_2$B$_9$H$_{10}$-10-SEt$_2$)]$^-$,[5] and the nickel complex [Ni(PPh$_3$)$_2$(η^5-7,8-C$_2$B$_9$H$_{11}$)] rearranges, thermally interchanging a PPh$_3$ group with the hydrogen atom of the β-BH vertex to yield [NiH(PPh$_3$)(η^5-7,8-C$_2$B$_9$H$_{10}$-10-PPh$_3$)].[6] Also relevant to substitution of hydrogen atoms at B-10 vertices are the numerous known di- and trimetallacarborane compounds where a B$_\beta$ vertex in the open CCB*B*B face of the *nido*-C$_2$B$_9$ cage ligating one metal center forms an exopolyhedral B–metal σ bond with an adjacent metal center.[3b]

The molybdenum atom in **2b** is also coordinated by two cisoid CO molecules as well as by the allyl group. The latter adopts an *exo*- rather than an *endo*-conformation. The former structure is also the most stable conformer of the complex [Mo(CO)$_2$(η^3-C$_3$H$_5$)(η^5-C$_5$H$_5$)].[7] The Mo–C(11) (2.342(4) Å), Mo–C(12) (2.234(4) Å), and Mo–C(13) (2.365(4) Å) distances for **2b** are very similar to the corresponding separations in [Mo(CO)$_2$(η^3-C$_3$H$_5$)(η^5-C$_5$H$_5$)], which are 2.359(3), 2.236(4), and 2.359(3) Å, respectively.[8] The C–C distances (1.404(4) and 1.409(5) Å) within the allyl group in **2b** show that the ligand is symmetrically bound in the η^3-fashion, a feature found also in [Mo(CO)$_2$(η^3-C$_3$H$_5$)(η^5-C$_5$H$_5$)] (C–C 1.380(4) Å).

The complexes **2** are thus zwitterionic in nature, with formally a positive charge on the donor atom attached to

---

(5) Hawthorne, M. F.; Warren, L. F.; Callahan, K. P.; Travers, N. F. *J. Am. Chem. Soc.* **1971**, *93*, 2407.

(6) King, R. E.; Miller, S. B.; Knobler, C. B.; Hawthorne, M. F. *Inorg. Chem.* **1983**, *22*, 3548.

(7) Davison, A.; Rode, W. C. *Inorg. Chem.* **1967**, *6*, 2125.

(8) Faller, J. W.; Chodosh, D. F.; Katahira, D. *J. Organomet. Chem.* **1980**, *187*, 227.

Table 3. Carbon-13 and Boron-11 NMR Data[a]

compd	^{13}C/δ	^{11}B/δ[b]
2a	237.6 (CO), 81.1 (CH), 77.2 (OCH$_2$), 47.7 (CH$_2$), 38.8 (br, cage CH), 13.1 (OCH$_2$*Me*)	22.8 (1 B, BOCH$_2$), −8.5 (2 B, BH), −15.7 (1 B, BH), −17.3 (2 B, BH), −20.9 (2 B, BH), −24.1 (1 B, BH)
2b	238.0 (CO), 79.7 (CH), 76.1 (OCH$_2$), 59.4 (br, *C*Me), 50.8 (CH$_2$), 26.6 (C*Me*), 12.8 (OCH$_2$*Me*)	23.6 (1 B, BOCH$_2$), −9.7 (2 B, BH), −12.6 (3 B, BH), −13.9 (2 B, BH), −16.5 (1 B, BH)
2c	227.5 (CO), 76.6 (O*C*H$_2$Me), 71.8 (CH), 57.3 (br, *C*Me), 42.4 (CH$_2$), 27.5 (C*Me*), 12.8 (OCH$_2$*Me*)	22.2 (1 B, BOCH$_2$), −9.3 (2 B, BH), −12.4 (3 B, BH), −13.9 (2 B, BH), −15.5 (1 B, BH)
2d[c]	238.7 (CO), 81.1 (OCH$_2$), 79.7 (CH), 60.3 (br, *C*Me), 50.8 (CH$_2$), 27.3 (C*Me*), 25.5 (OCH$_2$*C*H$_2$)	23.8 {1 B, BO(CH$_2$)$_4$}, −6.5 (2 B, BH), −9.0 (3 B, BH), −10.8 (2 B, BH), −13.5 (1 B, BH)
2e	236.7 (CO), 79.5 (CH$_2$), 63.2 (br, *C*Me), 51.7 (CH), 27.0 and 26.5 (C*Me* and SMe)	1.1 (1 B, BSMe$_2$), −7.9 (1 B, BH), −10.8 (4 B, BH), −12.8 (2 B, BH), −13.6 (1 B, BH)
2f[d]	235.9 (d, CO, *J*(PC) = 4), 134.9 to 128.5 (C$_6$H$_5$), 77.0 (CH), 64.6 (br, *C*Me), 51.6 (CH$_2$), 28.4 (C*Me*)	−4.1 (br, 1 B, BPPh$_3$), −7.8 (2 B, BH), −9.3 (3 B, BH), −12.1 (3 B, BH)
2g[d]	238.0 (CO), 144.4 to 126.0 (NC$_5$H$_5$), 79.7 (CH), 61.2 (br, *C*Me), 50.1 (CH$_2$), 26.6 (C*Me*)	11.7 (1 B, BNC$_5$H$_5$), −6.8 (2 B, BH), −10.4 (1 B, BH), −11.9 (2 B, BH), −13.1 (2 B, BH), −13.9 (1 B, BH)
2h	237.7 (CO), 151.4 to 121.5 (m, N$_2$C$_{10}$H$_8$), 80.0 (CH), 61.3 (br, *C*Me), 50.5 (CH$_2$), 26.5 (C*Me*)	11.6 (1 B, BN$_2$C$_{10}$H$_8$), −6.8 (3 B, BH), −11.9 (2 B, BH), −13.1 (2 B, BH), −13.3 (1 B, BH)
3a	240.8 (CO), 75.6 (CH), 63.7 (OCH$_2$), 59.1 (br, *C*Me), 53.0 (t, NCH$_2$, *J*(NC) = 3), 50.1 (CH$_2$), 30.2 (C*Me*), 17.8 (OCH$_2$*Me*), 7.7 (NCH$_2$*Me*)	20.1 (1 B, BOCH$_2$), −10.0 (4 B, BH), −16.1 (4 B, BH)
3b	231.9 (WCO, *J*(WC) = 160), 68.3 (CH), 63.9 (OCH$_2$), 57.4 (br, *C*Me), 53.0 (t, NCH$_2$, *J*(NC) = 3), 43.2 (CH$_2$), 32.5 (C*Me*), 17.7 (OCH$_2$*Me*), 7.7 (NCH$_2$*Me*)	18.5 (1 B, BOCH$_2$), −10.2 (4 B, BH), −15.0 (3 B, BH), −17.7 (1 B, BH)
3d[f]	240.7 (CO), 84.9 (d, CH$_2$F, *J*(FC) = 162), 75.5 (CH), 68.2 (OCH$_2$), 59.2 (br, NCH$_2$), 59.0 (br, *C*Me), 49.8 (CH$_2$), 30.3 (C*Me*), 27.9 and 27.7 (OCH$_2$*C*H$_2$*C*H$_2$), 24.1 (NCH$_2$*C*H$_2$), 19.9 (NCH$_2$CH$_2$*C*H$_2$), 13.6 (N(CH$_2$)$_3$*Me*)	20.1 (1 B, BOCH$_2$), −10.2 (4 B, BH), −16.0 (4 B, BH)
4a	221.0 (CO), 70.3 (br, *C*Me), 65.3 (OCH$_2$), 32.5 (C*Me*), 17.0 (OCH$_2$*Me*)	27.2 (1 B, BOCH$_2$), −2.8 (3 B, BH), −6.2 (4 B, BH), −10.7 (1 B, BH)
4b	221.9 (CO), 63.9 (OCH$_2$), 33.1 (C*Me*), 28.3 (C*Me*), 16.7 (OCH$_2$*Me*)	23.4 (1 B, BOCH$_2$), 0.6 (1 B, BH), −3.5 (2 B, BH), −6.7 (2 B, BH), −10.0 (1 B, BH), −11.4 (1 B, BH), −17.4 (1 B, BH)
4c	209.8 (WCO, *J*(WC) = 160), 65.6 (OCH$_2$), 64.9 (br, *C*Me), 33.0 (C*Me*), 17.0 (OCH$_2$*Me*)	24.0 (1 B, BOCH$_2$), −3.2 (3 B, BH), −7.5 (2 B, BH), −8.0 (2 B, BH), −10.2 (1 B, BH)
4d[g]	220.9 (CO), 84.4 (d, CH$_2$F, *J*(FC) = 160), 69.4 (OCH$_2$), 62.7 (br, *C*Me), 32.5 (C*Me*), 27.5 and 27.3 (OCH$_2$*C*H$_2$*C*H$_2$)	27.2 (1 B, BOCH$_2$), −2.9 (3 B, BH), −6.2 (4 B, BH), −10.5 (1 B, BH)
6a	387.6 (μ-C, *J*(WC) = 140), 232.4, 218.9, 218.0 (CO), 161.8 to 119.1 (C$_6$H$_4$), 94.0 (C$_5$H$_5$), 68.2 (br, *C*Me), 64.0 (br, *C*Me), 63.7 (OCH$_2$), 34.2 (C*Me*), 31.4 (C*Me*), 21.1 (Me-4), 17.0 (OCH$_2$*Me*)	18.2 (1 B, BOCH$_2$), 17.2 (1 B, BH), −2.7 (1 B, BH), −6.0 (1 B, BH), −9.8 (3 B, BH), −12.8 (1 B, BH), −14.2 (1 B, BH)
6b	382.4 (μ-C, *J*(WC) = 140), 234.3, 221.1, 220.3 (CO), 161.7 to 119.5 (C$_6$H$_4$), 93.6 (C$_5$H$_5$), 71.5 (br, *C*Me), 63.5 (OCH$_2$), 59.8 (br, *C*Me), 35.6 (C*Me*), 28.5 (C*Me*), 21.1 (Me-4), 17.0 (OCH$_2$*Me*)	25.1 (1 B, BOCH$_2$), 15.2 (1 B, BH), −7.0 (3 B, BH), −7.5 (1 B, BH), −9.5 (1 B, BH), −12.4 (1 B, BH), −16.0 (1 B, BH)

[a] Measured in CD$_2$Cl$_2$ at ambient temperatures, unless otherwise stated. Hydrogen-1 decoupled, chemical shifts are positive to high frequency of SiMe$_4$ (^{13}C) and BF$_3$·Et$_2$O (external) (^{11}B), respectively. *J* values given in Hz. [b] Signals ascribed to more than one nucleus may result from overlapping peaks and do not necessarily indicate symmetry equivalence. [c] Measured in acetone-*d*$_6$. [d] ^{31}P{^{1}H} NMR: δ 8.7 ppm (q, br, *J*(BP) = 140). [e] Measured in acetone-*d*$_6$–benzene-*d*$_6$ (1:1). [f] ^{19}F NMR: δ −64.0 ppm (t of t, CH$_2$F, *J*(HF) = 50). [g] ^{19}F NMR: δ −65.2 ppm (t of t, CH$_2$F, *J*(HF) = 50).

Table 4. Selected Internuclear Distances (Å) and Angles (deg) for [Mo(CO)$_2$(η^3-C$_3$H$_5$)(η^5-7,8-Me$_2$-7,8-C$_2$B$_9$H$_8$-10-OEt$_2$)] (2b), with Estimated Standard Deviations in Parentheses

Mo–C(1)	2.484(3)	Mo–C(2)	2.436(3)	Mo–B(3)	2.379(4)	Mo–B(4)	2.399(3)
Mo–B(5)	2.429(3)	Mo–C(9)	1.905(3)	Mo–C(10)	1.941(3)	Mo–C(11)	2.342(4)
Mo–C(12)	2.234(4)	Mo–C(13)	2.365(4)	C(1)–C(2)	1.619(4)	C(1)–B(5)	1.710(4)
C(1)–B(6)	1.723(5)	C(1)–B(10)	1.713(5)	C(1)–C(3)	1.538(4)	C(2)–B(3)	1.710(3)
C(2)–B(6)	1.744(5)	C(2)–B(7)	1.728(5)	C(2)–C(4)	1.533(4)	B(3)–B(4)	1.773(4)
B(3)–B(7)	1.783(5)	B(3)–B(8)	1.802(5)	B(4)–B(5)	1.787(4)	B(4)–B(8)	1.774(5)
B(4)–B(9)	1.794(5)	B(4)–O(1)	1.544(3)	B(5)–B(9)	1.801(5)	B(5)–B(10)	1.771(5)
B(6)–B(7)	1.749(5)	B(6)–B(10)	1.751(5)	B(6)–B(11)	1.742(5)	B(7)–B(8)	1.750(4)
B(7)–B(11)	1.767(5)	B(8)–B(9)	1.774(5)	B(8)–B(11)	1.770(5)	B(9)–B(10)	1.749(4)
B(9)–B(11)	1.761(5)	B(10)–B(11)	1.767(6)	O(1)–C(5)	1.466(4)	O(1)–C(7)	1.479(3)
C(5)–C(6)	1.502(5)	C(7)–C(8)	1.489(5)	C(9)–O(9)	1.172(4)	C(10)–O(10)	1.158(4)
C(11)–C(12)	1.404(4)	C(12)–C(13)	1.409(5)				
C(9)–Mo–C(10)	75.1(1)	C(9)–Mo–C(11)	71.9(1)	C(9)–Mo–C(12)	103.4(2)	C(10)–Mo–C(12)	103.5(1)
C(11)–Mo–C(12)	35.6(1)	C(10)–Mo–C(13)	69.7(1)	C(12)–Mo–C(13)	35.5(1)	C(2)–C(1)–B(5)	110.7(2)
Mo–C(1)–C(3)	108.7(2)	Mo–C(2)–C(4)	108.4(2)	Mo–B(4)–O(1)	110.3(2)	B(3)–B(4)–O(1)	124.4(2)
B(5)–B(4)–O(1)	125.2(2)	B(4)–O(1)–C(5)	120.3(2)	B(4)–O(1)–C(7)	119.7(2)	C(5)–O(1)–C(7)	117.7(2)
O(1)–C(5)–C(6)	112.3(3)	O(1)–C(7)–C(8)	112.4(3)	Mo–C(9)–O(9)	177.7(3)	Mo–C(10)–O(10)	175.4(3)
Mo–C(11)–C(12)	68.0(2)	Mo–C(12)–C(11)	76.4(2)	Mo–C(12)–C(13)	77.3(2)	Mo–C(13)–C(12)	67.1(2)

the B-10 vertex of the cage and a negative charge on the metal atom. The presence of the B$_\beta$–L group is clearly revealed in the ^{11}B{^{1}H} NMR spectra (Table 3) of the species **2a**–**2e**, **2g**, and **2h** by the appearance of a relatively deshielded resonance, with an intensity corresponding to a single boron nucleus, in the range δ 23.6–1.1 ppm, the remaining boron nuclei in each spectrum giving rise to the customary broad overlapping signals to higher field.[3a] Importantly, in the fully coupled ^{11}B NMR spectra of these complexes the resonances assigned to the boron atoms of the B–L groups are singlets, in contrast with the more shielded resonances of the B–H groups which are doublets due to ^{11}B–^{1}H coupling. However, in **2f** the resonance for the boron of the BPPh$_3$ group occurs at δ −4.1 ppm and is broad due to unresolved ^{11}B–^{31}P coupling. Although appreciably more shielded than those for the other BL fragments in the compounds **2**, the resonance for the $BPPh_3$ group of **2f** is nevertheless of comparable chemical shift to those observed for the $BPPh_3$ nucei in nickel complexes with an exopolyhedral cage triphenylphosphine group, e.g., δ -1.95 ppm for $[NiH(PPh_3)(\eta^5\text{-}7,8\text{-}C_2B_9H_{10}\text{-}10\text{-}PPh_3)]$.[6] The $^{31}P\{^1H\}$ NMR spectrum of **2f** displays a broad quartet resonance at δ 8.7 ppm [$J(BP)$ = 140 Hz].

The IR spectra of the complexes **2** all show two CO stretching bands (Table 1) in accord with the presence of one conformer, presumed to be the *exo*-allyl species,[1a] as determined by X-ray diffraction for **2b**. Although in the solid state **2b** is revealed to be asymmetric, the NMR data indicate that in solution dynamic behavior occurs. Thus in the $^{13}C\{^1H\}$ NMR spectrum (Table 3), measured at room temperature, there is one resonance for the two CO ligands (δ 238.0 ppm), one broad peak for the two cage-carbon vertices (δ 59.4 ppm), and one signal for the two methylene groups of the allyl ligand (δ 50.8 ppm), indicating an equivalence within these respective pairs of groups on the NMR time scale. Similar features are shown in the $^{13}C\{^1H\}$ NMR spectra of the other complexes **2** and may be accounted for by rotation of the carborane cage about an axis through the metal atom and the centroid of the pentagonal C_2B_3 ring coordinated to the metal. Significantly, measurement of the $^{13}C\{^1H\}$ and ^1H NMR spectra at -90 °C did not result in the appearance of additional resonances to those observed at room temperature, indicating this rotation is also prevalent at these temperatures.

The ^1H NMR spectra (Table 2) of all the complexes **2** display characteristic peaks for the allyl ligand. For **2b** there are two doublets-of-triplets at δ 1.22 ($J(HH)$ = 11 and 1 Hz) and 3.07 ppm ($J(HH)$ = 7 and 1 Hz), which may be assigned to the *anti*-protons (H_a) and *syn*-protons (H_s), respectively. The triplet-of-triplets resonance at δ 3.85 ppm ($J(HH)$ = 11 and 7 Hz), corresponding in intensity to a single proton, is attributable to the central methine proton (H_c).[1a] In the ^1H NMR spectra of **2b**–**2h**, the cage CMe groups give rise to a single peak, rather than two, in agreement with the dynamic behavior mentioned above.

The presence in the complexes **2a**–**2c** of tricoordinate oxygen atoms, carrying a positive charge, suggested that their $BOEt_2$ groups might be susceptible to nucleophilic attack by hydride or halide ions. Accordingly, treatment of CH_2Cl_2 solutions of **2b** with $K[BH\{CH(Me)(Et)\}_3]$, as a source of hydride, afforded a new complex identified as $[Mo(CO)_2(\eta^3\text{-}C_3H_5)(\eta^5\text{-}7,8\text{-}Me_2\text{-}7,8\text{-}C_2B_9H_8\text{-}10\text{-}OEt)]^-$, which was isolated and characterized as its tetraethylammonium salt **3a** following addition of $[NEt_4]Cl$. Formation of **3a** is presumably accompanied by release of ethane following cleavage of a C–O bond in **2b**. Interestingly, the product of this reaction was not **1b**, the precursor of **2b**, so evidently the hydride abstraction process which yielded **2b** was not reversed.

Similar C–O bond cleavage was observed on treatment of the compounds **2b** and **2c** with $[NEt_4][X]$ (X = Cl or F), processes evidently involving loss of ethyl chloride or fluoride. Thus, treatment of thf solutions of **2b** or **2c** with $[NEt_4]F$ gives the complexes $[NEt_4][M(CO)_2(\eta^3\text{-}C_3H_5)(\eta^5\text{-}7,8\text{-}Me_2\text{-}7,8\text{-}C_2B_9H_8\text{-}10\text{-}OEt)]$ (M = Mo (**3a**) or W (**3b**)), respectively, isolated as stable solids and characterized by the data in Tables 1–3. Similarly, **2d** in thf with $[NEt_4]F$ yields $[NEt_4][Mo(CO)_2(\eta^3\text{-}C_3H_5)\{\eta^5\text{-}7,8\text{-}Me_2\text{-}7,8\text{-}C_2B_9H_8\text{-}10\text{-}O(CH_2)_3CH_2F\}]$ (**3c**), but this species could only be isolated as an oil. Use of $[NBu^n_4]F$ instead of $[NEt_4]F$ gave the salt **3d** in a faster reaction, and in this instance the product could be isolated as a solid. No reaction occurred when KF was used instead of the ammonium salts. Since the complexes **3** are salts, the CO stretching bands in the IR spectra for the anions are at a somewhat lower frequency than those of the neutral species **2b**–**2d**. The NMR data (Tables 2 and 3) for the complexes **3a**–**3d** are in agreement with the formulations proposed. The presence of the cage substituent at B-10 is clearly indicated by the $^{11}B\{^1H\}$ NMR spectra with the appearance of resonances for a single boron nucleus in the range δ 18.5–20.3 ppm.[3a] Peaks in the ^1H and $^{13}C\{^1H\}$ NMR spectra are as expected, assuming dynamic behavior as discussed above for the complexes **2**. Thus for all the compounds **3** the $^{13}C\{^1H\}$ NMR spectra (Table 3) show only one peak for the cage–carbon vertices and one for their methyl substituents, indicating an apparent equivalence of the CMe fragments in these room temperature spectra.

The salts **3** are of interest because protonation should result in release of the allyl group as propene. Accordingly, a CO-saturated CH_2Cl_2 solution of **3a** was treated with $HBF_4 \cdot Et_2O$, and in this way the compound $[Mo(CO)_4(\eta^5\text{-}7,8\text{-}Me_2\text{-}7,8\text{-}C_2B_9H_8\text{-}10\text{-}OEt)]$ (**4a**) was isolated. A similar procedure using **3b** afforded the tungsten analog **4c**. Complex $[Mo(CO)_4\{\eta^5\text{-}7,8\text{-}Me_2\text{-}7,8\text{-}C_2B_9H_8\text{-}10\text{-}O(CH_2)_3CH_2F\}]$ (**4d**) was also prepared by protonating **3c** under an atmosphere of CO. The compounds **4a**, **4c**, and **4d** are closely related structurally to the complexes $[W(CO)_4(\eta^5\text{-}7,8\text{-}Me_2\text{-}7,8\text{-}C_2B_9H_8\text{-}10\text{-}CH_2R)]$ (R = alkyl or aryl), obtained[3a] by protonating salts of the anionic species $[W(\equiv CR)(CO)_2(\eta^5\text{-}7,8\text{-}Me_2\text{-}7,8\text{-}C_2B_9H_9)]^-$ with $HBF_4 \cdot Et_2O$, and to the complexes $[M(CO)_4(\eta^5\text{-}7,8\text{-}Me_2\text{-}7,8\text{-}C_2B_9H_9)]$ (M = Mo or W), similarly obtained from the reagents **1b** and **1c** in the presence of CO.[1a] Data characterizing **4a**, **4c** and **4d** are given in Tables 1–3.

During characterization of **4a**, it was found that, at room temperature, solutions of this complex isomerized over a period of a few hours to give the polytopal isomer $[Mo(CO)_4(\eta^5\text{-}2,8\text{-}Me_2\text{-}2,8\text{-}C_2B_9H_8\text{-}10\text{-}OEt)]$ (**4b**), which contains a 2,1,8-MoC_2B_9 icosahedral core, rather than the 3,1,2-MoC_2B_9 framework present in the precursor. Some decomposition to give $[Mo(CO)_6]$ was also observed. Indeed, in order to isolate pure **4a**, during work-up procedures column chromatography was carried out at -20 °C, at which temperature no isomerization or decomposition took place. This type of isomerization has previously been observed to occur readily with 3,1,2-MoC_2B_9 cage frameworks. Thus, protonation with aqueous HI of the anion of **1b**, as its $[N(PPh_3)_2]^+$ salt, yields initially $[N(PPh_3)_2][MoI(CO)_3(\eta^5\text{-}7,8\text{-}Me_2\text{-}7,8\text{-}C_2B_9H_9)]$, but this product at room temperature slowly isomerizes to $[N(PPh_3)_2][MoI(CO)_3(\eta^5\text{-}2,8\text{-}Me_2\text{-}2,8\text{-}C_2B_9H_9)]$.[1b] The structural change accompanying formation of **4b** from **4a** was revealed by spectroscopic measurements. Although **4a** and **4b** both have three CO stretching bands of very similar frequencies, these frequencies are nevertheless detectably different. Moreover, the ^1H NMR spectrum of **4b** (Table 2) displays two peaks at δ 1.51 and 1.76 ppm for the nonequivalent cage CMe groups in the asymmetric structure, whereas **4a** has one such peak (δ 2.22 ppm). Unfortunately, **4b** was isolated in relatively poor yield, and the $^{13}C\{^1H\}$ NMR spectrum (Table 3) was weak, so the two signals for the cage *C*Me nuclei were not observed. However, the expected two peaks for the C*Me* fragments were seen at δ 33.1 and 28.3 ppm. It may be noted that whether or not the *nido*-C_2B_9 fragment in **4b** is rotating about an axis through the molybdenum, the cage CMe fragments will remain nonequivalent.

4b

○ BH ◎ B ● CMe

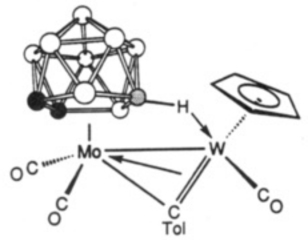

5a

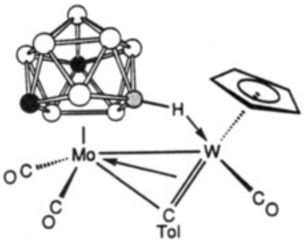

5b

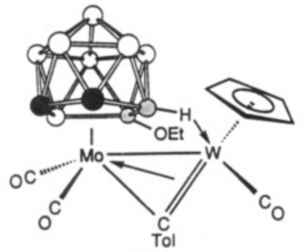

6a

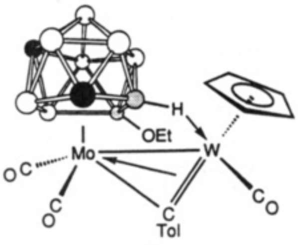

6b

Tol = C_6H_4Me-4

○ BH ○ B ● CMe

Interestingly, unlike **4a**, the tungsten analog **4c** does not isomerize and does not readily decompose in solution. This is in contrast to previous results with other systems where the skeletal rearrangements for molybdenum species have been observed to proceed more slowly than those for their tungsten analogs. Thus treatment of the $[N(PPh_3)_2]^+$ salt of the anion of **1c** with aqueous HI affords $[N(PPh_3)_2][WI(CO)_3(\eta^5\text{-}2,8\text{-}Me_2\text{-}2,8\text{-}C_2B_9H_9)]$.[1b] An intermediate with the 3,1,2-MC_2B_9 icosahedral geometry akin to $[N(PPh_3)_2][MoI(CO)_3(\eta^5\text{-}7,8\text{-}Me_2\text{-}7,8\text{-}C_2B_9H_9)]$ or **4c** was not observed. Evidently rearrangement of the icosahedral framework in these compounds is influenced by the nature of the ligands attached to the metal atoms and by the presence or absence of exopolyhedral substituents on the cage boron atoms. We suggest that the differing behavior of **4a** and **4c** may be due to CO dissociation occurring more readily for the former; the rearrangement of **4a** thus being initiated by loss of a CO ligand which is subsequently recovered from the solutions to yield the eventual product. This is further substantiated by the observation that, unlike **4a**, complex **4c** does not react readily with the electron donor $[W(\equiv CC_6H_4Me\text{-}4)(CO)_2(\eta^5\text{-}C_5H_5)]$ (see below), a process which would require the displacement of CO. It is noteworthy that two of the CO stretching frequencies of **4c** (2096, 2029, and 2002 cm^{-1}) are somewhat lower than those of **4a** (2096, 2037, and 2012 cm^{-1}), in accord with the CO ligands being more tightly bound in the tungsten compound.

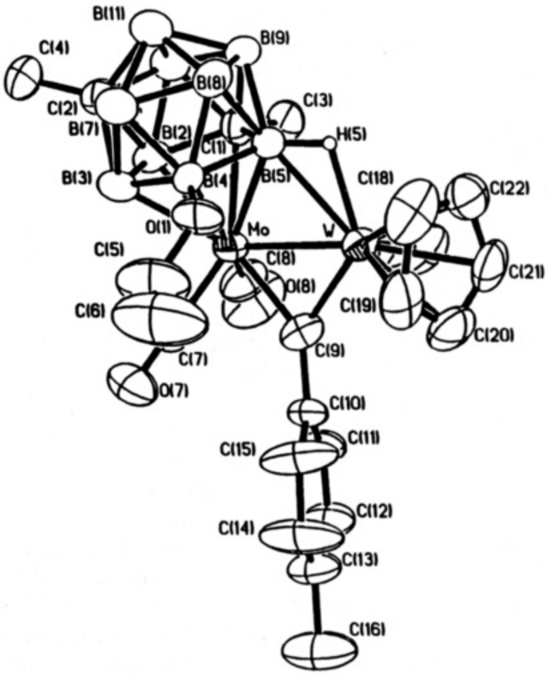

Figure 2. Structure of $[MoW(\mu\text{-}CC_6H_4Me\text{-}4)(CO)_3(\eta^5\text{-}C_5H_5)(\eta^5\text{-}2,8\text{-}Me_2\text{-}2,8\text{-}C_2B_9H_8\text{-}10\text{-}OEt)]$ (**6b**), showing the crystallographic labeling scheme.

It has been shown earlier[1b] that $[N(PPh_3)_2][MoI(CO)_3(\eta^5\text{-}7,8\text{-}Me_2\text{-}7,8\text{-}C_2B_9H_9)]$ upon treatment with $TlPF_6$ in the presence of $[W(\equiv CC_6H_4Me\text{-}4)(CO)_2(\eta^5\text{-}C_5H_5)]$ affords the dimetal complex $[MoW(\mu\text{-}CC_6H_4Me\text{-}4)(CO)_3(\eta^5\text{-}C_5H_5)(\eta^5\text{-}7,8\text{-}Me_2\text{-}7,8\text{-}C_2B_9H_9)]$ (**5a**) and that a similar reaction of $[N(PPh_3)_2][MoI(CO)_3(\eta^5\text{-}2,8\text{-}Me_2\text{-}2,8\text{-}C_2B_9H_9)]$ yields a mixture of **5a** and its isomer $[MoW(\mu\text{-}CC_6H_4Me\text{-}4)(CO)_3(\eta^5\text{-}C_5H_5)(\eta^5\text{-}2,8\text{-}Me_2\text{-}2,8\text{-}C_2B_9H_9)]$ (**5b**) in a ca. 1:3 ratio. In both isomeric complexes **5**, the Mo–W bond is spanned on one side by the *p*-tolylmethylidyne group and on the other by a three-center two-electron B–H ⇀ W bond, involving a BH vertex in the open pentagonal face of the *nido*-C_2B_9 cage ligating the molybdenum atom. It was therefore of interest to investigate reactions of the species **4a** and **4b** with $[W(\equiv CC_6H_4Me\text{-}4)(CO)_2(\eta^5\text{-}C_5H_5)]$. The presence of the exopolyhedral OEt substituents on the β-boron vertices in **4a** and **4b** opened the possibility that in any dimetal species formed the metal–metal bonds might be bridged by the OEt groups, forming a B–O(Et) ⇀ W linkage rather than an agostic B–H ⇀ W system.

Treatment of **4a** in CH_2Cl_2 at ambient temperatures with the alkylidynetungsten complex $[W(\equiv CC_6H_4Me\text{-}4)(CO)_2(\eta^5\text{-}C_5H_5)]$ affords $[MoW(\mu\text{-}CC_6H_4Me\text{-}4)(CO)_3(\eta^5\text{-}C_5H_5)(\eta^5\text{-}7,8\text{-}Me_2\text{-}7,8\text{-}C_2B_9H_8\text{-}10\text{-}OEt)]$ (**6a**), while the corresponding reaction with **4b** yields $[MoW(\mu\text{-}CC_6H_4Me\text{-}4)(CO)_3(\eta^5\text{-}C_5H_5)(\eta^5\text{-}2,8\text{-}Me_2\text{-}2,8\text{-}C_2B_9H_8\text{-}10\text{-}OEt)]$ (**6b**). Data characterizing these compounds are given in Tables 1–3, and a single-crystal X-ray structure determination was carried out on **6b**. The structure of the latter is shown in Figure 2, and important internuclear distances and angles are listed in Table 5.

The Mo–W bond is (as expected) spanned by the *p*-tolylmethylidyne ligand. The dimensions of the Mo(μ-C)W ring (Mo–W = 2.645(1), Mo–C(9) = 2.088(7), W–C(9) = 1.961(7) Å) in **6b** are comparable with those in $[MoW(\mu\text{-}CC_6H_4Me\text{-}4)(CO)_3(\eta^5\text{-}C_9H_7)(\eta^5\text{-}7,8\text{-}Me_2\text{-}7,8\text{-}C_2B_9H_9)]$ (C_9H_7 = indenyl) (Mo–W = 2.657(2), Mo–μ-C =

Table 5. Selected Internuclear Distances (Å) and Angles (deg) for $[MoW(\mu\text{-}CC_6H_4Me\text{-}4)(CO)_3(\eta^5\text{-}C_5H_5)(\eta^5\text{-}2,8\text{-}Me_2\text{-}2,8\text{-}C_2B_9H_8\text{-}10\text{-}OEt)]$ (6b)

Mo–W	2.645(1)	Mo–C(1)	2.337(7)	Mo–B(2)	2.357(9)	Mo–B(3)	2.395(9)
Mo–B(4)	2.443(8)	Mo–B(5)	2.251(9)	Mo–C(7)	1.984(8)	Mo–C(8)	2.004(9)
Mo–C(9)	2.088(7)	W–B(5)	2.415(9)	W–H(5)	1.87	W–C(9)	1.961(7)
W–C(17)	1.931(8)	C(1)–C(3)	1.54(1)	B(4)–O(1)	1.41(1)	C(2)–C(4)	1.51(1)
O(1)–C(5)	1.39(1)	C(5)–C(6)	1.40(2)	C(1)–B(2)	1.72(1)	C(1)–B(5)	1.76(1)
C(1)–B(9)	1.73(1)	C(1)–B(10)	1.70(1)	C(1)–C(3)	1.54(1)	B(2)–B(3)	1.78(1)
B(2)–C(2)	1.73(1)	B(2)–B(10)	1.80(1)	B(3)–B(4)	1.80(1)	B(3)–C(2)	1.75(1)
B(3)–B(7)	1.77(1)	B(4)–B(5)	1.88(1)	B(4)–B(7)	1.76(1)	B(4)–B(8)	1.80(1)
B(5)–H(5)	1.11	B(5)–B(8)	1.80(1)	B(5)–B(9)	1.77(1)	C(2)–B(7)	1.69(1)
C(2)–B(10)	1.68(1)	C(2)–B(11)	1.72(1)	B(7)–B(8)	1.77(1)	B(7)–B(11)	1.76(1)
B(8)–B(9)	1.75(1)	B(8)–B(11)	1.77(1)	B(9)–B(10)	1.77(1)	B(9)–B(11)	1.74(1)
B(10)–B(11)	1.75(1)	C(7)–O(7)	1.14(1)	C(8)–O(8)	1.13(1)	C(9)–C(10)	1.446(9)
C(13)–C(16)	1.50(1)						
C(1)–Mo–B(4)	76.7(3)	C(7)–Mo–C(8)	82.2(4)	C(7)–Mo–C(9)	76.1(3)	C(8)–Mo–C(9)	91.0(3)
C(1)–Mo–W	92.5(2)	B(4)–Mo–W	80.1(2)	B(5)–Mo–W	58.4(2)	C(9)–Mo–W	47.2(2)
Mo–B(5)–W	69.0(2)	H(5)–B(5)–W	48.3(2)	B(5)–H(5)–W	105.4(3)	B(4)–O(1)–C(5)	118.8(7)
Mo–C(7)–O(7)	178.4(7)	Mo–C(8)–O(8)	176.3(8)	Mo–C(9)–C(10)	138.3(5)	Mo–C(9)–W	81.5(2)
W–C(9)–C(10)	140.2(6)	W–C(17)–O(17)	174.2(7)				

1.95(2), W–μ-C = 2.03(2) Å)[9] and in $[MoW(\mu\text{-}CC_6H_4Me\text{-}4)(CO)_2(PMe_3)(\eta^5\text{-}C_5H_5)(\eta^5\text{-}7,9\text{-}Me_2\text{-}7,9\text{-}C_2B_{10}H_{10})]$ (Mo–W = 2.702(1), Mo–μ-C 1.94(1), W–μ-C = 2.10(1) Å),[10] where the carborane cages are coordinated to the tungsten atoms and where the indenyl and cyclopentadienyl groups are bonded to the molybdenums, respectively. These three molecules are formally 32 valence electron dimetal species, and in accord with their electronic unsaturation the metal–metal bonds are appreciably shorter than those in the electronically saturated 34 valence electron complexes $[MoW\{\mu\text{-}C(C_6H_4OMe\text{-}2)C(Me)O\}(CO)_4(\eta^5\text{-}C_5H_5)_2]$ (2.935(1) Å)[11] and $[MoW\{\mu\text{-}\eta^3{:}\eta^2\text{-}C(Bu^t)CC[{=}C(H)C_6H_4\text{-}Me\text{-}4]\}(CO)_4(\eta^5\text{-}C_5H_5)(\eta^5\text{-}7,8\text{-}C_2B_9H_{11})]$ (3.031(2) Å),[12] the latter containing $W(\eta^5\text{-}7,8\text{-}C_2B_9H_{11})$ and $Mo(\eta^5\text{-}C_5H_5)$ fragments bridged by a μ-C_3 moiety. However, as discussed elsewhere,[13] electronically unsaturated dimetal molybdenum–tungsten species are known which have relatively long metal–metal distances comparable with those found in molecules with 34 valence electrons, so it is evident that the steric and bonding requirements of the bridging groups also influence these separations.

The molecule **6b** contains a B–H ⇀ W bridge involving B(5), the boron vertex in the pentagonal ring coordinated to the molybdenum which lies between carbon atom C(3) and the boron atom B(4) carrying the OEt substituent. Thus B–H ⇀ W bridge bonding in this molecule is preferred over a B–O(Et) → W linkage, even though a lone pair of electrons is available on the oxygen to relieve the electron deficiency. The site of the bridging hydrogen ligand H(5) is based on potential-energy minimization calculations,[14] but the parameters W–H(5) (1.87 Å) and W–B(5) (2.415(9) Å) compare favorably with those in $[W_2(\mu\text{-}CC_6H_4Me\text{-}4)(CO)_3(\eta^5\text{-}C_5H_5)(\eta^5\text{-}7,9\text{-}Me_2\text{-}7,9\text{-}C_2B_9H_9)]$ (W–H = 2.05(6), W–B = 2.481(5) Å)[10] and $[W_2(\mu\text{-}CC_6H_4Me\text{-}4)(CO)_2\{N_2C(C_6H_4Me\text{-}4)_2\}(\eta^5\text{-}C_9H_7)(\eta^5\text{-}7,8\text{-}Me_2\text{-}7,8\text{-}C_2B_9H_9)]$ (W–H = 1.87(4), W–B = 2.470(6) Å),[15] where the μ-H groups of the B–H ⇀ W linkages were directly located and refined.

The X-ray structural analysis of **6b** clearly reveals that the molybdenum atom, C(1), C(2), and the nine boron atoms form a 2,1,8-MoC_2B_9 icosahedral framework. As expected, the molybdenum atom is coordinated by two CO molecules as well as the cage, and the tungsten atom carries the C_5H_5 ring and a CO group. Thus the structure of **6b** is very similar to that of **5b**, differing in that the latter has an exopolyhedral OEt substituent.

Complex **6a** did not isomerize into **6b** after heating at reflux in thf for several hours. This is of interest in view of the observation that the complex $[MoW(\mu\text{-}CC_6H_4Me\text{-}4)(CO)_3(\eta^5\text{-}C_9H_7)(\eta^5\text{-}7,8\text{-}Me_2\text{-}7,8\text{-}C_2B_9H_9)]$ isomerizes to $[MoW(\mu\text{-}CC_6H_4Me\text{-}4)(CO)_3(\eta^5\text{-}C_9H_7)(\eta^5\text{-}7,9\text{-}Me_2\text{-}7,9\text{-}C_2B_9H_9)]$ on heating in solvents for several hours.[9]

The spectroscopic data for the complexes **6** are in accord with their formulations. Both isomers display in the IR spectra three CO stretching bands. The ^1H NMR spectra (Table 2) unequivocally establish the presence of the B–H ⇀ W groups with quartet resonances at δ −7.52 (**6a**) and −8.27 ppm (**6b**). The J(BH) couplings (ca. 60 Hz) are diagnostic for such groups, as are the signals in the $^{11}B\{^1H\}$ NMR spectra at δ 18.2 (**6a**) and 25.1 ppm (**6b**).[3a] The asymmetric structures result in the cage CMe groups displaying two resonances in the ^1H NMR spectra, and these are at δ 1.97 and 2.19 ppm for **6a** and at δ 1.57 and 1.91 ppm for **6b**. Correspondingly, the $^{13}C\{^1H\}$ NMR spectrum (Table 3) of each isomer shows four signals for these groups: **6a**, δ 68.2, 64.0 (*C*Me), and 34.2, 31.4 ppm (C*Me*); **6b**, δ 71.5, 59.8 (*C*Me), and 35.6, 28.5 ppm (C*Me*). The spectra also as expected display three resonances for the CO ligands.

Resonances in the $^{13}C\{^1H\}$ NMR spectra for the bridging carbon atoms of the alkylidyne ligands are seen at δ 387.6 (**6a**) and 382.4 ppm (**6b**), with J(WC) = 140 Hz. These signals may be compared with those observed in the spectra of **5a** and **5b**, at δ 380.1 and 384.2 ppm, respectively.[1a,b] The chemical shifts for the μ-C nuclei for all four compounds **5** and **6** are relatively deshielded and occur in the range found for many μ-alkylidyne–dimetal complexes which are electronically unsaturated with 32 valence electrons.[16] Formally, the $(\eta^5\text{-}C_5H_5)(CO)W{\equiv}CC_6H_4Me\text{-}4$ units in **5** and **6** may be regarded as contributing four electrons to the molybdenum atoms so as to give these

---

[9] Green, M.; Howard, J. A. K.; James, A. P.; Jelfs, A. N. de M.; Nunn, C. M.; Stone, F. G. A. *J. Chem. Soc., Dalton Trans.* **1987**, 81.

[10] Brew, S. A.; Carr, N.; Mortimer, M. D.; Stone, F. G. A. *J. Chem. Soc., Dalton Trans.* **1991**, 811.

[11] Hart, I. J.; Jeffery, J. C.; Lowry, R. M.; Stone, F. G. A. *Angew. Chem., Int. Ed. Engl.* **1988**, *27*, 1703.

[12] Bruce, G. C.; Mullica, D. F.; Sappenfield, E. L.; Stone, F. G. A. *J. Chem. Soc., Dalton Trans.* **1992**, 2685.

[13] Dossett, S. J.; Hart, I. J.; Pilotti, M. U.; Stone, F. G. A. *J. Chem. Soc., Dalton Trans.* **1991**, 511.

[14] Orpen, A. G. *J. Chem. Soc., Dalton Trans.* **1980**, 2509.

[15] Howard, J. A. K.; James, A. P.; Jelfs, A. N. de M.; Nunn, C. M.; Stone, F. G. A. *J. Chem. Soc., Dalton Trans.* **1987**, 1221.

[16] (a) Brew, S. A.; Dossett, S. J.; Jeffery, J. C.; Stone, F. G. A. *J. Chem. Soc., Dalton Trans.* **1990**, 3709. (b) Dossett, S. J.; Hart, I. J.; Stone, F. G. A. *J. Chem. Soc., Dalton Trans.* **1990**, 3481. (c) Dossett, S. J.; Hill, A. F.; Jeffery, J. C.; Marken, F.; Sherwood, P.; Stone, F. G. A. *J. Chem. Soc., Dalton Trans.* **1988**, 2453.

metal centers a filled valence shell. However, as discussed elsewhere there are several alternative ways to represent the electron distribution in the Mo(μ-C)W rings in these compounds.[16a]

Conclusions

Hydride abstraction from the compounds **1** is thus specifically associated with the proton attached to the β-boron atom of the η^5-C_2B_3 ring of the carborane cage. Significantly, the allyl moiety of these complexes is not the preferred site of loss of hydride, in contrast to the related cyclopentadienylmolybdenum allyl species $[Mo(CO)_2(\eta^3\text{-}C_3H_4Me)(\eta^5\text{-}C_5H_5)]$,[17] which loses a hydride from the allyl group on reaction with $[CPh_3][BF_4]$. The complexes **2** belong to a class of compounds containing monoanionic carborane ligands of the general type $[LC_2B_9H_8R_2]^-$, where L is a 2e⁻ donor. Ligands of this type are significant because they are formally more closely related to $C_5H_5^-$ than the now widely quoted $[C_2B_9H_9R_2]^{2-}$; in spite of this, relatively few examples of the ligands $[LC_2B_9H_8R_2]^-$ have appeared in the literature.[18] The species **2** thus have extended the range of compounds containing ligands of this type. Furthermore, novel types of alkoxide-substituted carborane ligands are produced as a result of C–O bond cleavage of the ether substituent attached to the carborane cage framework of complexes **2a–2d** by the nucleophiles X^- (X = H, F, or Cl).

Experimental Section

General Considerations. Solvents were distilled from appropriate drying agents under nitrogen prior to use. Petroleum ether refers to that fraction of boiling point 40–60 °C. All reactions were carried out under an atmosphere of dry nitrogen using Schlenk line techniques. Chromatography columns (ca. 15 cm in length and ca. 2 cm in diameter, unless otherwise stated) were packed with alumina (Brockmann activity II) or with silica gel (Aldrich, 70–230 mesh). The compounds $[NEt_4][M(CO)_2(\eta^3\text{-}C_3H_5)(\eta^5\text{-}7,8\text{-}R_2\text{-}7,8\text{-}C_2B_9H_9)]$ (M = Mo or W, R = H or Me)[1] and $[W(\equiv CC_6H_4Me\text{-}4)(CO)_2(\eta^5\text{-}C_5H_5)]$[19] were prepared as previously described. The reagents $[CPh_3][BF_4]$, $[NEt_4]F\cdot xH_2O$, and $[NEt_4]Cl\cdot xH_2O$ were purchased from Aldrich Chemical Co. and used without further purification. K-selectride and $[NBu^n_4]F$ were 1.0 M solutions in thf, as supplied by Aldrich. Tetrafluoroboric acid was an 85% solution of $HBF_4\cdot OEt_2$ in OEt_2, as supplied by Aldrich. The NMR spectra were recorded in CD_2Cl_2 at ambient temperatures, unless otherwise stated, at the following frequencies: ^1H at 360.13 MHz, ^{13}C at 90.56 MHz, ^{31}P at 145.78 MHz, ^{11}B at 115.55 MHz, and ^{19}F at 84.25 MHz.

Synthesis of the Complexes $[M(CO)_2(\eta^3\text{-}C_3H_5)(\eta^5\text{-}7,8\text{-}R_2\text{-}7,8\text{-}C_2B_9H_8\text{-}10\text{-}L)]$ (2). (i) A CH_2Cl_2 solution (10 mL) of $[NEt_4][Mo(CO)_2(\eta^3\text{-}C_3H_5)(\eta^5\text{-}7,8\text{-}C_2B_9H_{11})]$ (**1a**) (0.25 g, 0.55 mmol), to which OEt_2 (ca. 0.5 mL) had been added, was treated with solid $[CPh_3][BF_4]$ (0.20 g, 0.60 mmol) at −78 °C. Immediately the solution darkened to a brown–yellow color. The reaction mixture was warmed to room temperature, after which it was stirred for 20 min. Solvent was removed in vacuo, the residue extracted with CH_2Cl_2–petroleum ether (1:1, 3 mL), and the extract chromatographed on alumina. Elution with CH_2Cl_2–petroleum ether (1:4) yielded a single yellow band which was collected. Solvent was removed in vacuo and the residue crystallized from CH_2Cl_2–petroleum ether (1:5, 2 mL) to give yellow *microcrystals* of $[Mo(CO)_2(\eta^3\text{-}C_3H_5)(\eta^5\text{-}7,8\text{-}C_2B_9H_{10}\text{-}10\text{-}OEt_2)]$ (**2a**) (0.16 g).

(ii) Similarly, treatment of a CH_2Cl_2 solution (10 mL) of $[NEt_4][Mo(CO)_2(\eta^3\text{-}C_3H_5)(\eta^5\text{-}7,8\text{-}Me_2\text{-}7,8\text{-}C_2B_9H_9)]$ (**1b**) (0.25 g, 0.52 mmol) with $[CPh_3][BF_4]$ (0.18 g, 0.55 mmol) in the presence of OEt_2 (ca. 0.5 mL) at −78 °C afforded yellow *microcrystals* of $[Mo(CO)_2(\eta^3\text{-}C_3H_5)(\eta^5\text{-}7,8\text{-}Me_2\text{-}7,8\text{-}C_2B_9H_8\text{-}10\text{-}OEt_2)]$ (**2b**) (0.15 g).

(iii) Employing $[NEt_4][W(CO)_2(\eta^3\text{-}C_3H_5)(\eta^5\text{-}7,8\text{-}Me_2\text{-}7,8\text{-}C_2B_9H_9)]$ (**1c**) (0.30 g, 0.54 mmol), $[CPh_3][BF_4]$ (0.20 g, 0.60 mmol) and OEt_2 (ca. 0.5 mL) afforded yellow *microcrystals* of $[W(CO)_2(\eta^3\text{-}C_3H_5)(\eta^5\text{-}7,8\text{-}Me_2\text{-}7,8\text{-}C_2B_9H_8\text{-}10\text{-}OEt_2)]$ (**2c**) (0.21 g).

(iv) Similarly, treatment of a CH_2Cl_2 solution (10 mL) of **1b** (0.25 g, 0.52 mmol) with $[CPh_3][BF_4]$ (0.18 g, 0.55 mmol) in the presence of thf (ca. 0.5 mL) at −78 °C afforded yellow *microcrystals* of $[Mo(CO)_2(\eta^3\text{-}C_3H_5)(\eta^5\text{-}7,8\text{-}Me_2\text{-}7,8\text{-}C_2B_9H_8\text{-}10\text{-}OC_4H_8)]$ (**2d**) (0.15 g).

(v) The reaction of **1b** (0.25 g, 0.52 mmol) with $[CPh_3][BF_4]$ (0.18 g, 0.55 mmol) in the presence of SMe_2 (ca. 0.5 mL) at −78 °C afforded yellow *microcrystals* of $[Mo(CO)_2(\eta^3\text{-}C_3H_5)(\eta^5\text{-}7,8\text{-}Me_2\text{-}7,8\text{-}C_2B_9H_8\text{-}10\text{-}SMe_2)]$ (**2e**) (0.08 g).

(vi) The salt **1b** (0.25 g, 0.52 mmol) and PPh_3 (0.31 g, 1.2 mmol) were dissolved in CH_2Cl_2 (20 mL), and the solution was cooled to ca. −78 °C. Solid $[CPh_3][BF_4]$ (0.20 g, 0.60 mmol) was added, and the solution was allowed to warm to room temperature. Stirring was continued for a further 20 min, after which the solution was preadsorbed onto alumina and transferred to the top of an alumina chromatography column. Elution with CH_2Cl_2–petroleum ether (1:1) gave an orange solution which was reduced in volume in vacuo to ca. 5 mL. Petroleum ether (10 mL) was added and the mixture set aside at −20 °C for 15 h to give orange *microcrystals* of $[Mo(CO)_2(\eta^3\text{-}C_3H_5)(\eta^5\text{-}7,8\text{-}Me_2\text{-}7,8\text{-}C_2B_9H_8\text{-}10\text{-}PPh_3)]$ (**2f**) (0.14 g).

(vii) Employing a similar procedure to that described for the preparation of **2f**, the salt **1b** (0.25 g, 0.52 mmol), pyridine (ca. 0.5 mL), and $[CPh_3][BF_4]$ (0.20 g, 0.60 mmol) afforded yellow *microcrystals* of $[Mo(CO)_2(\eta^3\text{-}C_3H_5)(\eta^5\text{-}7,8\text{-}Me_2\text{-}7,8\text{-}C_2B_9H_8\text{-}10\text{-}NC_5H_5)]$ (**2g**) (0.10 g).

(viii) Similarly, **1b** (0.25 g, 0.52 mmol), 4,4′-bipyridine (0.14 g, 1.0 mmol), and $[CPh_3][BF_4]$ (0.20 g, 0.60 mmol) afforded orange *microcrystals* of $[Mo(CO)_2(\eta^3\text{-}C_3H_5)(\eta^5\text{-}7,8\text{-}Me_2\text{-}7,8\text{-}C_2B_9H_8\text{-}10\text{-}NC_5H_4C_5H_4N)]$ (**2h**) (0.09 g).

Synthesis of the Salts $[NR_4][M(CO)_2(\eta^3\text{-}C_3H_5)(\eta^5\text{-}7,8\text{-}Me_2\text{-}7,8\text{-}C_2B_9H_8\text{-}10\text{-}OR')]$ (3). (i) A CH_2Cl_2 solution (20 mL) of $[Mo(CO)_2(\eta^3\text{-}C_3H_5)(\eta^5\text{-}7,8\text{-}Me_2\text{-}7,8\text{-}C_2B_9H_8\text{-}10\text{-}OEt_2)]$ (**2b**) (0.10 g, 0.24 mmol) was treated with an excess of $K[BH\{CH(Me)(Et)\}_3]$ (ca. 1.0 mL, 1.0 mmol), and the mixture was stirred at room temperature for 6 h, after which $[NEt_4]Cl$ (ca. 0.2 g) was added. The solution was preadsorbed onto alumina and transferred to an alumina chromatography column (ca. 5 cm in length). Elution initially with CH_2Cl_2–petroleum ether (1:1) removed traces of unreacted **2b**. Further elution with CH_2Cl_2–thf (10:1) gave a yellow eluate. Solvent was removed in vacuo, and the residue was washed with OEt_2 (3 × 5 mL) and then crystallized from CH_2Cl_2–OEt_2 (1:1, 5 mL) to give yellow *microcrystals* of $[NEt_4][Mo(CO)_2(\eta^3\text{-}C_3H_5)(\eta^5\text{-}7,8\text{-}Me_2\text{-}7,8\text{-}C_2B_9H_8\text{-}10\text{-}OEt)]$ (**3a**) (0.06 g).

(ii) A thf (20 mL) solution of $[Mo(CO)_2(\eta^3\text{-}C_3H_5)(\eta^5\text{-}7,8\text{-}Me_2\text{-}7,8\text{-}C_2B_9H_8\text{-}10\text{-}OEt_2)]$ (**2b**) (0.20 g, 0.47 mmol) was treated with solid $[NEt_4]F$ (0.20 g, 1.3 mmol), and the mixture was stirred at room temperature for 4 h. Solvent was removed in vacuo, the residue was extracted with CH_2Cl_2 (ca. 5 mL), and the solution was preadsorbed onto alumina and transferred to an alumina chromatography column (ca. 5 cm in length). Yellow *microcrystals* of **3a** (0.18 g) were obtained by following the same procedure as described above.

(iii) Using a similar procedure, the reaction between **2c** (0.25 g, 0.49 mmol) and $[NEt_4]F$ (0.20 g, 1.3 mmol) in thf (20 mL) yielded yellow *microcrystals* of $[NEt_4][W(CO)_2(\eta^3\text{-}C_3H_5)(\eta^5\text{-}7,8\text{-}Me_2\text{-}7,8\text{-}C_2B_9H_8\text{-}10\text{-}OEt)]$ (**3b**) (0.20 g).

(iv) Following a similar procedure to that described for **3a**, the reaction between **2d** (0.20 g, 0.47 mmol) and $[NEt_4]F$ (0.20 g, 1.3 mmol) in thf (20 mL) yielded, after column chromatography, a yellow oil (0.18 g) which was washed with diethyl ether (3 × 5 mL) and dried in vacuo. The yellow oil was identified as $[NEt_4]$-

---

[17] Faller, J. W.; Rosan, A. M. *J. Am. Chem. Soc.* **1977**, *99*, 4858.

[18] Douek, N. L.; Welch, A. J. *J. Chem. Soc., Dalton Trans.* **1993**, 1917 and references cited therein.

[19] Fischer, E. O.; Lindner, T. L.; Huttner, G.; Freidrich, P.; Kreissl, F. R.; Besenhard, J. O. *Chem. Ber.* **1977**, *110*, 3397.

[$Mo(CO)_2(\eta^3\text{-}C_3H_5)\{\eta^5\text{-}7,8\text{-}Me_2\text{-}7,8\text{-}C_2B_9H_8\text{-}10\text{-}O(CH_2)_3CH_2F\}$] (**3c**) by means of infrared and ^1H, $^{11}B\{^1H\}$, $^{13}C\{^1H\}$, and ^{19}F NMR spectroscopy.

(v) Similarly, the reaction of **2d** (0.20 g, 0.47 mmol) with [NBu^n_4]F (0.10 mL, 1 M solution in thf, 0.10 mmol) gave yellow *microcrystals* of [NBu^n_4][$Mo(CO)_2(\eta^3\text{-}C_3H_5)\{\eta^5\text{-}7,8\text{-}Me_2\text{-}7,8\text{-}C_2B_9H_8\text{-}10\text{-}O(CH_2)_3CH_2F\}$] (**3d**) (0.17 g).

Protonation Reactions of the Salts [NEt_4][$M(CO)_2(\eta^3\text{-}C_3H_5)(\eta^5\text{-}7,8\text{-}Me_2\text{-}7,8\text{-}C_2B_9H_8\text{-}10\text{-}OR'$)] (3). (i) A CH_2Cl_2 (20 mL) solution of compound **3a** (0.15 g, 0.28 mmol) was saturated with CO at −78 °C. To this solution was added $HBF_4{\cdot}OEt_2$ (0.04 mL, 0.30 mmol), and the mixture was then stirred at room temperature for 15 min, with the CO source maintained. The resulting yellow solution was evaporated to dryness in vacuo and the residue extracted with CH_2Cl_2–petroleum ether (1:2, 3 mL). The extract was transferred to the top of a silica gel chromatography column held at −20 °C. Elution with the same solvent mixture gave a yellow solution from which the solvent was removed in vacuo at −20 °C to give [$Mo(CO)_4(\eta^5\text{-}7,8\text{-}Me_2\text{-}7,8\text{-}C_2B_9H_8\text{-}10\text{-}OEt$)] (**4a**) (0.05 g) as a yellow powder. This compound was characterized by means of infrared and ^1H, $^{11}B\{^1H\}$, and $^{13}C\{^1H\}$ NMR spectroscopy.

(ii) Employing a similar procedure to that described for **4a**, treatment of the salt **3b** (0.20 g, 0.33 mmol) with $HBF_4{\cdot}OEt_2$ (0.05 mL, 0.37 mmol) under an atmosphere of CO at −78 °C afforded yellow *microcrystals* of [$W(CO)_4(\eta^5\text{-}7,8\text{-}Me_2\text{-}7,8\text{-}C_2B_9H_8\text{-}10\text{-}OEt$)] (**4c**) (0.09 g) after crystallization from CH_2Cl_2–petroleum ether (1:3, 5 mL).

(iii) Similarly, treatment of **3c** (0.15 g, 0.26 mmol) with $HBF_4{\cdot}OEt_2$ (0.04 mL, 0.30 mmol), under an atmosphere of CO at −78 °C gave [$Mo(CO)_4\{\eta^5\text{-}7,8\text{-}Me_2\text{-}7,8\text{-}C_2B_9H_8\text{-}10\text{-}O(CH_2)_3CH_2F\}$] (**4d**) (0.05 g) as a yellow powder.

Synthesis of [$Mo(CO)_4(\eta^5\text{-}2,8\text{-}Me_2\text{-}2,8\text{-}C_2B_9H_8\text{-}10\text{-}OEt$)] (4b). Essentially pure **4a** (0.10 g, 0.24 mmol), obtained as described above, was dissolved in CH_2Cl_2 (5 mL), and the resulting solution was stirred at room temperature for 15 h, after which petroleum ether was added (3 mL) and the material transferred to the top of a silica gel chromatography column held at −20 °C. Eluting the column with CH_2Cl_2–petroleum ether (1:2) gave a pale yellow–brown fraction, containing [$Mo(CO)_6$], along with a yellow fraction. Solvent from the latter was removed in vacuo to afford [$Mo(CO)_4(\eta^5\text{-}2,8\text{-}Me_2\text{-}2,8\text{-}C_2B_9H_8\text{-}10\text{-}OEt$)] (**4b**) (0.02 g) as a yellow powder.

Synthesis of [$MoW(\mu\text{-}CC_6H_4Me\text{-}4)(CO)_3(\eta^5\text{-}C_5H_5)(\eta^5\text{-}7,8\text{-}Me_2\text{-}7,8\text{-}C_2B_9H_8\text{-}10\text{-}OEt$)] (6a). A freshly prepared sample of [$Mo(CO)_4(\eta^5\text{-}7,8\text{-}Me_2\text{-}7,8\text{-}C_2B_9H_8\text{-}10\text{-}OEt$)] (**4a**) (0.10 g, 0.24 mmol) and [$W(\equiv CC_6H_4Me\text{-}4)(CO)_2(\eta^5\text{-}C_5H_5)$] (0.12 g, 0.30 mmol) were dissolved in CH_2Cl_2 (10 mL), and the mixture was stirred at room temperature for 1.5 h. The resultant green solution was transferred to the top of an alumina chromatography column. Elution with CH_2Cl_2–petroleum ether (2:1) yielded a green band which was collected. After removal of the solvent in vacuo, the residue was crystallized from CH_2Cl_2–petroleum ether (1:2, 5 mL) to give green *microcrystals* of [$MoW(\mu\text{-}CC_6H_4Me\text{-}4)(CO)_3(\eta^5\text{-}C_5H_5)(\eta^5\text{-}7,8\text{-}Me_2\text{-}7,8\text{-}C_2B_9H_8\text{-}10\text{-}OEt$)] (**6a**) (0.08 g).

Synthesis of [$MoW(\mu\text{-}CC_6H_4Me\text{-}4)(CO)_3(\eta^5\text{-}C_5H_5)(\eta^5\text{-}2,8\text{-}Me_2\text{-}2,8\text{-}C_2B_9H_8\text{-}10\text{-}OEt$)] (6b). In a similar experiment as described for **6a**, a sample of freshly prepared **4a** (0.10 g, 0.24 mmol) was dissolved in CH_2Cl_2 (10 mL) and the solution stirred at room temperature for 4 h, thereby generating **4b**. Solid [$W(\equiv CC_6H_4Me\text{-}4)(CO)_2(\eta^5\text{-}C_5H_5)$] (0.12 g, 0.30 mmol) was then added and the mixture stirred for a further 1.5 h. The resultant green solution was transferred to the top of an alumina chromatography column. Elution with CH_2Cl_2–petroleum ether (2:1) yielded two green fractions, the latter of which was shown by IR and NMR measurements to be **6a**. Solvent from the other green eluate was removed in vacuo, and the residue was crystallized from CH_2Cl_2–petroleum ether (1:2, 3 mL) to give green *microcrystals* of [$MoW(\mu\text{-}CC_6H_4Me\text{-}4)(CO)_3(\eta^5\text{-}C_5H_5)(\eta^5\text{-}2,8\text{-}Me_2\text{-}2,8\text{-}C_2B_9H_8\text{-}10\text{-}OEt$)] (**6b**) (0.06 g).

Table 6. Data for X-ray Crystal Structure Analyses[a]

	2b	**6b**
crystal dimens/mm	0.12 × 0.30 × 0.41	0.16 × 0.30 × 0.46
formula	$C_{13}H_{29}B_9MoO_3$	$C_{22}H_{31}B_9MoO_4W$
M_r	426.6	736.5
cryst color, shape	yellow, parallelopiped	green, irregular shape
cryst system	triclinic	monoclinic
space group (No.)	$P\bar{1}$ (No. 2)	$C2/c$ (No. 15)
a/Å	7.106(1)	28.763(3)
b/Å	9.088(2)	10.950(3)
c/Å	16.271(2)	18.030(1)
α/deg	75.08(1)	
β/deg	92.77(1)	94.785(7)
γ/deg	102.19(1)	
V/Å^3	992.4(2)	5659(2)
Z	2	8
d_{calcd}/g cm^{-3}	1.430	1.729
μ(Mo–K$_\alpha$)/cm^{-1}	6.54	46.1
F(000)/e	436	2848
2θ range/deg	3–45	3–40
T/K	292	292
no. of reflns measd	2837	3310
no. of unique reflns	2585	2637
no. of observed reflns	2379	2367
criterion for observed n [$F_0 \geq n\sigma(F_o)$]	$n = 6$	$n = 4$
R, (R')[b]	0.0243, (0.0278)	0.0297, (0.0338)
final electron density diff features (max./min.)/eÅ^{-3}	0.39/−0.26	1.00/−0.72
S (goodness-of-fit)	1.11	1.29

[a] Data collected on an Enraf Nonius CAD4-F automated diffractometer operating in the ω–2θ scan mode (h, 0 to 7; k, −9 to 9; l, −17 to 17 for **2b**; h, 0 to 27; k, 0 to 10; l, −17 to 17 for **6b**); graphite monochromated Mo K$_\alpha$ X-radiation, $\bar{\lambda}$ = 0.710 73 Å. Refinement was by block full matrix least-squares on F with a weighting scheme of the form $w^{-1} = [\sigma^2(F_o) + g|F_o|^2]$ (g = 0.0006 for **2b**, 0.0005 for **6b**) where $\sigma_c{}^2(F_o)$ is the variance in F_o due to counting statistics. [b] $R = \sum||F_o| - |F_c||/\sum|F_o|$, $R' = \sum w^{1/2}||F_o| - |F_c||/\sum w^{1/2}|F_o|$.

Table 7. Atomic Coordinates (×10^4) and Equivalent Isotropic Displacement Parameters (Å^2 × 10^3) for 2b

name	x	y	z	U(eq)[a]
Mo	2239(1)	1228(1)	1603(1)	29(1)
C(1)	4289(4)	3272(3)	2201(2)	34(1)
C(2)	2140(4)	3606(3)	2013(2)	35(1)
B(3)	429(4)	2058(3)	2526(2)	33(1)
B(4)	1722(4)	660(3)	3108(2)	29(1)
B(5)	4206(4)	1446(3)	2846(2)	33(1)
B(6)	3587(5)	4509(4)	2714(3)	44(1)
B(7)	1139(5)	3735(4)	2933(2)	44(1)
B(8)	917(5)	1894(4)	3639(2)	41(1)
B(9)	3266(5)	1515(4)	3841(2)	39(1)
B(10)	4891(5)	3117(4)	3248(2)	44(1)
B(11)	2878(5)	3405(4)	3736(3)	50(1)
C(3)	5933(4)	4162(4)	1569(2)	49(1)
C(4)	1729(4)	4826(3)	1218(2)	52(1)
O(1)	833(3)	−1082(2)	3464(1)	34(1)
C(5)	2071(4)	−2226(3)	3688(2)	45(1)
C(6)	2325(5)	−2768(4)	4632(2)	60(1)
C(7)	−1151(4)	−1556(3)	3811(2)	52(1)
C(8)	−2175(5)	−3074(4)	3665(3)	72(1)
C(9)	355(5)	−619(4)	1630(2)	55(1)
O(9)	−825(4)	−1753(4)	1673(2)	96(1)
C(10)	567(4)	1802(4)	648(2)	53(1)
O(10)	−531(4)	2123(4)	117(2)	86(1)
C(11)	3821(5)	−669(4)	1402(2)	62(1)
C(12)	4791(5)	842(4)	1000(2)	57(1)
C(13)	3906(5)	1717(4)	306(2)	62(1)

[a] Equivalent isotropic U defined as one-third of the trace of the orthogonalized U_{ij} tensor.

Crystal Structure Determinations and Refinements. The crystal data and other experimental details for the compounds [$Mo(CO)_2(\eta^3\text{-}C_3H_5)(\eta^5\text{-}7,8\text{-}C_2B_9H_8\text{-}10\text{-}OEt_2$)] (**2b**) and [$MoW(\mu\text{-}CC_6H_4Me\text{-}4)(CO)_3(\eta^5\text{-}C_5H_5)(\eta^5\text{-}2,8\text{-}Me_2\text{-}2,8\text{-}C_2B_9H_8\text{-}10\text{-}OEt$)] (**6b**) are presented in Table 6. Crystals of **2b** and **6b** were grown by slow diffusion from a CH_2Cl_2–petroleum ether solution. Using a Zeiss Photomicroscope II, conoscopic examinations of both

Table 8. Atomic Coordinates ($\times 10^4$) and Equivalent Isotropic Displacement Parameters ($Å^2 \times 10^3$) for 6b

name	*x*	*y*	*z*	*U*(eq)[a]
Mo	3934(1)	3254(1)	2643(1)	38(1)
C(1)	3590(2)	4315(6)	1615(4)	45(2)
B(2)	4062(3)	3482(8)	1376(5)	48(2)
B(3)	3960(3)	1919(8)	1595(5)	47(2)
B(4)	3418(3)	1736(7)	2015(5)	39(2)
B(5)	3211(3)	3361(7)	2064(5)	38(2)
C(2)	3807(3)	2512(7)	706(4)	52(2)
B(7)	3444(3)	1483(8)	1056(5)	49(2)
B(8)	2972(3)	2332(8)	1357(5)	48(2)
B(9)	3071(3)	3860(8)	1136(4)	47(2)
B(10)	3600(3)	3950(9)	703(5)	56(2)
B(11)	3216(3)	2723(9)	521(5)	55(2)
C(3)	3616(3)	5704(6)	1726(4)	59(2)
C(4)	4104(3)	2157(8)	90(4)	62(2)
O(1)	3267(2)	801(4)	2470(3)	55(2)
C(5)	3590(3)	−42(9)	2767(6)	97(2)
C(6)	3402(5)	−1001(11)	3157(8)	150(2)
C(7)	4456(3)	2187(8)	3034(4)	59(2)
O(7)	4748(2)	1553(6)	3253(4)	92(2)
C(8)	4410(3)	4565(9)	2879(4)	70(2)
O(8)	4664(3)	5331(7)	3039(4)	114(2)
C(9)	3824(3)	3034(6)	3765(4)	44(2)
C(10)	4091(3)	2720(7)	4454(4)	44(2)
C(11)	4408(3)	3505(6)	4798(5)	59(2)
C(12)	4660(3)	3227(7)	5462(5)	68(2)
C(13)	4631(3)	2113(7)	5781(4)	68(2)
C(14)	4306(5)	1336(9)	5449(6)	122(2)
C(15)	4034(4)	1632(8)	4800(5)	101(2)
C(16)	4908(4)	1775(9)	6494(6)	114(2)
W	3191(1)	3526(1)	3397(1)	41(1)
C(17)	3396(3)	5200(8)	3512(4)	61(2)
O(17)	3521(3)	6193(6)	3647(3)	92(2)
C(18)	2491(3)	2562(10)	3520(5)	85(2)
C(19)	2831(3)	2172(9)	4128(5)	80(2)
C(20)	2934(3)	3158(10)	4578(5)	76(2)
C(21)	2677(3)	4128(10)	4274(5)	73(2)
C(22)	2413(3)	3787(9)	3638(5)	67(2)

[a] Equivalent isotropic *U* defined as one-third of the trace of the orthogonalized U_{ij} tensor.

systems verified their optical homogeneity and biaxial nature. For each data set, final unit cell parameters were obtained from the setting angle values of 25 accurately centered reflections. Periodic intensity measurements of three control reflections for each compound, monitored at 2-h intervals of collection time, revealed no sign of deterioration. Thus, the electronic hardware reliability and crystal stability were confirmed. After removal of these check reflections, the data for each complex were corrected for Lorentz, polarization, and X-ray absorption effects. The latter corrections were based on an empirical method employing high-angle ψ scan data. The data of **2b** and **6b** were averaged (R_{int} = 0.010 (**2b**), 0.038 (**6b**)), and an additional examination of each data set using an $N(Z)$ analysis (cumulative probability distribution test) provided evidence that both systems were centrosymmetric and that neither possessed higher symmetry.[20]

Crystallographic analyses (direct methods for **2b** and the heavy atom Patterson method for **6b**) of the reduced and averaged data revealed the location of all non-hydrogen atoms. Regarding **6b**, the hydrogen H(5) was located by employing the program XHYDEX.[14] All other hydrogen atoms in compound **6b** and all hydrogen atoms in compound **2b** were included at geometrically calculated positions (C–H 0.96 Å and B–H 1.10 Å) using a riding model with fixed isotropic thermal parameters (U_{iso} = 80 and 60 $\times 10^{-3}$ Å^2, respectively). All calculations were performed using the SHELXTL-PC package of programs.[21] Atomic scattering factors with related anomalous dispersion correction factors were obtained from the usual source.[22] Final atomic positional parameters for non-hydrogen atoms are given in Tables 7 and 8.

Acknowledgment. We thank the Robert A. Welch Foundation for support (Grants AA-1201 and -0668), and the South African Foundation for Research Development for a postdoctoral bursary (to S.F.W.).

Supplementary Material Available: Complete tables of bond lengths and angles, anisotropic thermal parameters, and hydrogen atom parameters for **2b** and **6b** (13 pages). Ordering information is given on any current masthead page.

OM9306640

---

(20) Howells, E. R.; Phillips, D. C.; Rogers, D. *Acta Crystallogr.* **1950**, *3*, 210.

(21) Siemens (1989). SHELXTL-PC Siemens X-ray Instruments, Madison WI.

(22) *International Tables for X-ray Crystallography*; Kynoch Press; Birmingham, UK, 1974; Vol. 4.